

1 Isotopic evidence for biogenic molecular hydrogen production in 2 the Atlantic Ocean

3 S. Walter^{1*}, A. Kock², T. Steinhoff², B. Fiedler², P. Fietzek^{2,5}, J. Kaiser³, M. Krol¹, M.
4 E. Popa¹, Q. Chen⁴, T. Tanhua², and T. Röckmann¹

5 [1] Institute for Marine and Atmospheric Research (IMAU), Utrecht University, The
6 Netherlands

7 * now Energy research Center of the Netherlands (ECN), Petten, The Netherlands

8 [2] Marine Biogeochemistry, GEOMAR/Helmholtz-Centre for Ocean Research, Kiel,
9 Germany

10 [3] Centre for Ocean and Atmospheric Sciences, School of Environmental Sciences,
11 University of East Anglia, Norwich, NR4 7TJ, United Kingdom

12 [4] Department of Atmospheric Sciences, University of Washington, Seattle, Washington,
13 USA

14 [5] Kongsberg Maritime Contros GmbH, Kiel, Germany

15

16 Correspondence to: S. Walter (s.walter@uu.nl)

17

18 Abstract

19 Oceans are a net source of molecular hydrogen (H₂) to the atmosphere. The production of
20 marine H₂ is assumed to be mainly biological by N₂ fixation, but photochemical pathways are
21 also discussed. We present measurements of mole fraction and isotopic composition of
22 dissolved and atmospheric H₂ from the southern and northern Atlantic between 2008 and
23 2010. In total almost 400 samples were taken during five cruises along a transect between
24 Punta Arenas (Chile) and Bremerhaven (Germany), as well as at the coast of [Mauritania](#).

25 The isotopic source signatures of dissolved H₂ extracted from surface water are highly
26 deuterium-depleted and correlate negatively with temperature, showing δD values of (-
27 629±54) ‰ for water temperatures at (27±3) °C and (-249±88) ‰ below (19±1) °C. The
28 results for warmer water masses are consistent with biological production of H₂. This is the

Sylvia Walter 20.12.2015 21:33

Style Definition: Equation: Font:Times
New Roman, English (UK), Justified,
Space After: 6 pt

Sylvia Walter 20.12.2015 21:33

Deleted: Mauretania

1 first time that marine H₂ excess has been directly attributed to biological production by
2 isotope measurements. However, the isotope values obtained in the colder water masses
3 indicate that beside possible biological production a significant different source should be
4 considered.

5 The atmospheric measurements show distinct differences between both hemispheres as well
6 as between seasons. Results from the global chemistry transport model TM5 reproduce the
7 measured H₂ mole fractions and isotopic composition well. The climatological global oceanic
8 emissions from the GEMS database are in line with our data and previously published flux
9 calculations. The good agreement between measurements and model results demonstrates that
10 both the magnitude and the isotopic signature of the main components of the marine H₂ cycle
11 are in general adequately represented in current atmospheric models despite a proposed
12 source different from biological production or a substantial underestimation of nitrogen
13 fixation by several authors.

14

15 **1 Introduction**

16 Molecular hydrogen (H₂) is the second most abundant reduced compound in the atmosphere
17 after methane (CH₄). H₂ is not a radiatively active gas itself, but – via its role in atmospheric
18 chemistry – it indirectly influences the lifetime of the greenhouse gas CH₄ and several air
19 pollutants (Prather, 2003; Schultz et al., 2003; Tromp et al., 2003; Warwick et al., 2004;
20 Jacobson, 2008; Feck et al., 2008; Ehhalt and Rohrer, 2009, Popa et al. 2015). The main H₂
21 sources are photo-oxidation of CH₄ and non-methane volatile organic compounds (NMVOC)
22 in the atmosphere and combustion processes at the surface, whereas soil deposition and
23 oxidation by hydroxyl radicals (HO[•]) are the main sinks. Oceans are a minor but significant
24 source to the global H₂ budget with a mean estimated contribution of 7 %. However,
25 estimates of the oceanic contribution range from 1 % to 15 % in different studies, indicating
26 high uncertainties (Novelli et al., 1999; Hauglustaine and Ehhalt, 2002; Ehhalt and Rohrer,
27 2009, and references herein, Pieterse et al. 2013).

28 Oceanic H₂ production is assumed to be mainly biological, as a by-product of nitrogen (N₂)
29 fixation (e.g. Conrad, 1988; Conrad and Seiler, 1988; Moore et al. 2009, 2014). H₂ is
30 produced during N₂ fixation in equimolar proportions, but also reused as an energy source.
31 The H₂ net production rate during N₂ fixation depends on environmental conditions and also
32 on microbial species (Bothe et al., 1980; 2010; Tamagnini et al., 2007; et al. 2010a). Besides

1 N₂ fixation, abiotic photochemical production from chromophoric dissolved organic matter
2 (CDOM) and small organic compounds such as acetaldehyde or syringic acid has also been
3 found to be a source of hydrogen in the oceans (Punshon and Moore, 2008a, and references
4 therein).

5 Unfortunately, measurements that constrain the temporal and spatial patterns of oceanic H₂
6 emissions to the atmosphere are sparse. Vertical profiles display highest concentrations in the
7 surface layer (up to 3 nmol L⁻¹) and a sharp decrease with depth towards undersaturation,
8 where the reasons for the undersaturation are not fully understood yet (e.g. Herr et al., 1981;
9 Scranton et al., 1982; Conrad & Seiler 1988). Tropical and subtropical surface waters are
10 supersaturated up to 10 times or even more with respect to atmospheric H₂ equilibrium
11 concentrations, and therefore a source of H₂ to the atmosphere. This is in contrast to temperate
12 and polar surface waters, which are generally undersaturated in H₂ (Scranton et al., 1982; Herr
13 et al., 1984; Herr, 1984; Conrad and Seiler, 1988; Seiler and Schmidt, 1974; Herr et al., 1981;
14 Lilley et al. 1982, Punshon et al., 2007, Moore et al. 2014).

15 Additional information to constrain the global H₂ budget and to gain insight into production
16 pathways comes from the analysis of the H₂ isotopic composition (quantitatively expressed as
17 isotope delta value, δD, see section 2.2). Different sources produce H₂ with characteristic δD
18 values. Moreover, the kinetic isotope fractionation in the two main removal processes, soil
19 deposition and reaction with HO[•], is different. The combined action of sources and sinks leads
20 to tropospheric H₂ with a δD of +130 ‰ relative to Vienna Standard Mean Ocean water
21 (VSMOW), (Gerst and Quay, 2001; Rhee et al., 2006; Rice et al., 2010; Batenburg et al.,
22 2011). In sharp contrast, surface emissions of H₂ from fossil fuel combustion and biomass
23 burning have δD values of approximately -200 ‰ and -300 ‰, respectively (Gerst and Quay,
24 2001; Rahn et al., 2002; Röckmann et al., 2010a; Vollmer et al., 2010). As originally
25 proposed by Gerst and Quay (2001), isotopic budget calculations require the photochemical
26 sources of H₂ to be enriched in deuterium, with δD values between +100 ‰ and +200 ‰
27 (Rahn et al., 2003; Röckmann et al., 2003; Feilberg et al., 2007; Nilsson et al., 2007; Pieterse
28 et al., 2009; Nilsson et al., 2010; Röckmann et al., 2010b). Biologically produced H₂ has the
29 most exceptional isotopic composition with δD of approximately -700 ‰ (Walter et al. 2012),
30 reflecting strong preference of biogenic sources for the lighter isotope ¹H.

31 The aim of the study was I) to determine the δD of dissolved H₂ and gain more information
32 about possible sources, and II) to get a high-resolution picture of the distribution of

1 atmospheric H₂ along meridional Atlantic transects during different seasons and compare it
2 with global model results. Samples were taken on four cruises along meridional Atlantic
3 transects in the southern and northern hemisphere and on one cruise at the coast of
4 [Mauritania](#). A total of almost 400 atmospheric and 22 ocean surface water samples were
5 taken, covering two seasons between 2008 and 2010.

6 **2 Methods**

7 **2.1 Cruise tracks**

8 During four cruises of RV *Polarstern* and one of RV *L'Atalante* between February 2008 and
9 May 2010, air and seawater samples were collected (see Fig. 1, Table 1). The cruises of RV
10 *Polarstern* were part of the OCEANET project (Autonomous measuring platforms for the
11 regulation of substances and energy exchange between ocean and atmosphere, Hanschmann et
12 al. 2012).

13 They covered both hemispheres, between Punta Arenas (Chile, 53° S / 71° W) and
14 Bremerhaven (Germany, 53° N / 8° E). South–north transects were carried out in boreal
15 spring (April / May) and north–south transects in boreal autumn (October / November). The
16 transects followed similar tracks as the Atlantic Meridional Transect (AMT) programme
17 (<http://amt-uk.org/>) and crossed a wide range of ecosystems and oceanic regimes, from sub-
18 polar to tropical and from euphotic shelf seas and upwelling systems to oligotrophic mid-
19 ocean gyres (Robinson et al. 2009, Longhurst 1998).

20 The RV *L'Atalante* followed a cruise track from Dakar (Senegal) to Mindelo (Cape Verde),
21 covering a sampling area along the coast of Mauritania and a transect to the Cape Verde
22 Islands. This area is characterized by strongly differing hydrographical and biological
23 properties with an intensive seasonal upwelling. Area and cruise track are described in more
24 detail in Walter et al. (2013) and Kock et al. (2008).

25

26 **2.2 Atmospheric air sampling**

27 Discrete atmospheric air samples were taken on–board RV *Polarstern* at the bridge deck,
28 using 1 L borosilicate glass flasks coated with black shrink-hose (NORMAG), with 2 Kel-F
29 (PCTFE) O–ring sealed valves. The flasks were pre–conditioned by flushing with N₂ at 50 °C
30 for at least 12 hours; the N₂ remained in the flask at ambient pressure until the sampling.
31 During sampling the flasks were flushed for 4 minutes with ambient air at a flow rate of 12 L
32 min⁻¹ using Teflon tubes and a membrane pump (KNF VERDER PM22874–86 N86ANDC).

Sylvia Walter 20.12.2015 21:33

Deleted: Mauretania

1 The sample air was dried with Drierite® (CaSO₄). The flasks were finally pressurized to
2 approximately 1.7 bar, which allows duplicate measurements of the H₂ isotopic composition
3 of an air sample.

4 Table 1 gives an overview of the sampling scheme for discrete H₂ samples. In total 360
5 samples were collected, regularly distributed over the transects at 4 to 6 hour intervals. In
6 2009 the resolution of sampling was enhanced to one sample per two hours and focused on
7 five sub-sections of the transect, in an attempt to resolve diel variability.

8 Samples were always taken at the downwind side of the ship to exclude a possible
9 contamination by ship diesel exhaust. One atmospheric sample was taken directly inside the
10 ship's funnel of RV *Polarstern* to determine the mole fraction and δD of ship diesel exhaust as
11 a possible contamination source. This first measurements for ship diesel exhaust gave an H₂
12 mole fraction of (930.6±3.2) nmol mol⁻¹ and a δD of (-228.6±5.0) ‰. In the following, we
13 will use the abbreviation "ppb" = 10⁻⁹ in place of the SI unit "nmol mol⁻¹".
14

15 **2.3 Headspace sampling from surface waters**

16 In addition to the atmospheric air samples, 16 headspace samples from surface water were
17 taken during the RV *Polarstern* cruise ANT-XXVI/4 in April / May 2010 and 6 samples
18 during the RV *L'Atalante* cruise in February 2008. The experimental setup (Fig. 2) was a
19 prototype, and deployed for the first time to extract headspace air from surface water for
20 isotopic composition measurements of molecular H₂. It consists of a glass vessel (10 L) and
21 an evacuation / headspace sampling unit.

22 The glass vessel was evacuated for at least 24 h before sampling, using a Pfeiffer vacuum
23 DUO 2.5A pump, with a capacity of 40 L min⁻¹ (STP: 20° C and 1 bar). Water samples were
24 taken from 5 m depth (RV *Polarstern* cruises) or 10 m depth (RV *L'Atalante* cruise) using a
25 24-Niskin-bottle rosette with a volume of 12 L each. Sampling started immediately after
26 return of the bottle rosette on-board and from a bottle dedicated to the H₂ measurements. The
27 evacuated glass vessel was connected to the Niskin bottle by Teflon tubing, which was first
28 rinsed with approximately 1 L surface water. Then, 8.4 L water streamed into the evacuated
29 flask (Fig. 2), using a drip to enhance the dispersion of the sample water. After connection of
30 the headspace-sampling unit, the lines were first evacuated and then flushed with a makeup
31 gas several times. During the RV *L'Atalante* cruise a synthetic air mixture with an H₂ mixing
32 ratio below threshold was used as makeup gas. The makeup gas used during the RV

1 *Polarstern* cruises was a synthetic air mixture with an H₂ mole fraction of (543.9±0.3) ppb
2 and a δD of (93.1±0.2) ‰. The mole fraction of the makeup gas was determined by the Max
3 Planck Institute for Biogeochemistry and is given on the MPI2009 scale (Jordan and
4 Steinberg, 2011). The glass vessel was pressurized to approximately 1.7 bar absolute with the
5 makeup gas and the total headspace (added makeup gas plus extracted gas from the water
6 sample) was then flushed to a pre-evacuated sample flask. The flasks were of the same type
7 as for the atmospheric sampling: 1 L borosilicate glass flasks (NORMAG), coated with black
8 shrink-hose to minimize photochemical reactions inside and sealed with 2 Kel-F (PCTFE) O-
9 ring sealed valves. All flasks were previously conditioned by flushing with N₂ at 50 °C for at
10 least 12 hours and evacuated for at least 12 hours directly before use. The whole sampling
11 procedure took around 15 minutes: (4.0±0.5) min flushing surface water to the evacuated
12 glass vessel, (8.0±1.0) min to connect the glass vessel to the sampling unit and evacuate the
13 lines, and (3.0±0.5) min to add and pressurize the glass vessel with the makeup gas and take
14 the headspace sample. The surface water temperature was on average (0.9±0.6) °C higher
15 than the air temperature. Given that most of the apparatus was at air temperature and that the
16 headspace will adjust to ambient temperature relatively quickly during equilibration the air
17 temperature was used for calculations. Since the temperature dependence of H₂ solubility is
18 less than 0.3 % per K for seawater between 16 °C and 30 °C (as encountered here) and view of
19 the large H₂ saturations (see below), the error associated with this assumption is negligible.
20 Flasks were stored in the dark until measurement. At the same location of headspace sampling
21 also atmospheric samples were taken (Table 4).

22

23 2.4 Measurements

24 2.4.1 Atmospheric H₂ and δD (H₂) in discrete samples

25 The mole fraction and isotopic composition of molecular H₂ was determined using the
26 experimental setup developed by Rhee et al. (2004) and described in detail in Walter et al.
27 (2012, 2013) and Batenburg et al. (2011). The D/¹H molar ratio in a sample, $R_{\text{sample}}(\text{D}/\text{H})$, is
28 quantified as the relative deviation from the D/¹H molar ratio in a standard, $R_{\text{standard}}(\text{D}/\text{H})$, as
29 isotope delta δD value, and reported in per mill (‰):

30

$$31 \delta D = \frac{R_{\text{sample}}(\text{D}/\text{H})}{R_{\text{standard}}(\text{D}/\text{H})} - 1 \quad (1)$$

32

Sylvia Walter 20.12.2015 21:33

Deleted: supersaturations

1 The isotopic standard is Vienna Standard Mean Ocean Water (VSMOW). H₂ mole fractions
2 are reported as mole fractions in nmol mol⁻¹, abbreviated ppb (10⁻⁹, parts per billion) and
3 linked to the MPI2009 calibration scale for atmospheric hydrogen (Jordan and Steinberg,
4 2011). As working standards, atmospheric air from laboratory reference air cylinders and
5 synthetic air mixtures were used (Walter et al. 2012, 2013, Batenburg et al. 2011); the H₂
6 mole fractions of the air in these cylinders were determined by the Max Planck Institute for
7 Biogeochemistry, Jena, Germany. The atmospheric reference air and the synthetic isotope
8 reference air were measured daily (atmospheric reference air at least twice) and results were
9 used for correction of the sample measurements. The uncertainties reported here reflect
10 random (i.e. repeatability) errors only and do not include possible systematic errors
11 (Batenburg et al., 2011; Walter et al., 2012, 2013). Samples were measured in random order
12 and analysed within 3 months (ANT-XXIV/4, ANT-XXV/5, ANT-XXVI/1) up to two years
13 (ANT-XXVI/4) after sampling. Storage tests indicate that glass flasks equipped with Kel-F
14 valves are stable for H₂ (Jordan and Steinberg, 2011). The mean measurement repeatability
15 between the two measurements on the same flask was between ±3.2 ppb (ANT-XXV/5, *n* =
16 14) and ±6.4 ppb (ANT-XXVI/4, *n* = 108) for the mole fraction and ±3.4 ‰ (ANT-XXVI/4, *n*
17 = 108) and ±5.0 ‰ (ANT-XXV/5, *n* = 14) for the isotopic composition.

18 H₂ and CO mole fractions were also measured by using a Peak Performer 1 RGA with
19 synthetic air as a carrier gas, either continuously on-board (ANT-XXVI/4, see section 2.4.2)
20 or from discrete flasks in the laboratory (ANT-XXV/5 and ANT-XXVI/1). The discrete RGA
21 measurements were performed from the same glass flasks after measurement of the isotope
22 system (see above). Due to a remaining slight overpressure in the flasks, an active pumping of
23 the air into the RGA was not necessary and the flasks were simply connected to the RGA inlet
24 by Teflon tubing. The remaining pressure was mostly sufficient to perform 8 to 10
25 measurements. A slight memory effect was observed and thus only the last 5 measurements
26 were taken into account when stable. Samples with only three or less valid measurements
27 were not used for evaluation. The standards were the same as those used for the isotope
28 system. For both cruises (ANT-XXV/5 and ANT-XXVI/1), the mean measurement
29 repeatability was better than ±0.8 % (H₂) and ±2 % (CO). A comparison between the H₂ mole
30 fractions measured with the Peak Performer 1 RGA and the isotopic experimental setup
31 reveals on average slightly lower RGA values of (7.5±23.8) ppb (see Fig. 3).

32

2.4.2 Atmospheric H₂ measured continuously

For the on-board continuous measurements of H₂ mole fractions a Peak Performer 1 RGA was used. The atmospheric air was drawn from the bridge deck to the laboratory in ¼ inch Decabon tubing. The CO mole fraction was also measured in the same measurement and will be reported here for information, but without further discussion.

In alternating order, 10 air samples and 10 aliquots of reference air were measured, using synthetic air as carrier gas. Due to small memory effects, only the last 5 measurements of each were taken into account when the values were stable. The mole fractions of H₂ and CO were calculated by using the mean of the enclosing standard measurements, with an estimated maximal error of ±5 %. For more details see Popa et al. 2014. The mean measurement repeatability for the air samples was ±1.7 % for H₂ and ±3.6 % for CO in ambient air, respectively ±0.8 % (H₂) and ±0.9 % (CO) for the reference air. Comparing the H₂ mole fractions measured continuously on the RGA with discrete samples measured on the isotope system and collected close in time, we found a mean offset of (-18.8±16.4) ppb for the RGA results.

16

2.4.3 Dissolved H₂ extracted from surface water

The discrete samples of extracted dissolved H₂ were measured as described for the discrete atmospheric samples in section 2.4.1. Details about assumptions and calculations to determine dissolved H₂ concentrations and isotope delta values and quantity symbols are given in detail in the Appendix.

Defining the extraction efficiency η as

$$\eta = \frac{c_h V_h}{c_{w0} V_w} \quad (2)$$

where V_h and V_w are the volume of the headspace and the water fraction, and c_h the concentration of H₂ in the headspace. The initial concentration of H₂ in seawater, c_{w0} , can be calculated from

$$c_{w0} = \frac{c_h V_h}{\eta V_w} \quad (3)$$

Sylvia Walter 20.12.2015 21:33

Deleted: $\eta = \frac{c_h V_h}{c_{w0} V_w}$

Sylvia Walter 20.12.2015 21:33

Formatted: Left, Space After: 0 pt

Sylvia Walter 20.12.2015 21:33

Formatted: Font:Not Italic

Sylvia Walter 20.12.2015 21:33

Formatted: Left, Space After: 0 pt, Line spacing: 1.5 lines

Sylvia Walter 20.12.2015 21:33

Formatted: Font:Not Italic

Sylvia Walter 20.12.2015 21:33

Deleted: $c_{w0} = \frac{c_h V_h}{\eta V_w}$

Sylvia Walter 20.12.2015 21:33

Formatted: Left, Space After: 0 pt

1 The concentration in the headspace, c_h , was not measured directly, but can be derived from
 2 the measured H_2 mole fraction in the sampling flask. The sampling procedure following gas
 3 extraction under vacuum can be broken into three steps (see Methods section):

- 4 1. Expansion of the headspace into the gas transfer system
- 5 2. Addition of makeup gas
- 6 3. Expansion of the headspace / makeup gas mixture into a sample flask

7 As shown in the Appendix, the original concentration of H_2 in seawater (in $nmol L^{-1}$) can be
 8 calculated using the following equation

9

$$10 \quad c_{w0} = \frac{y_f \left[\left(1 + \frac{V_t}{V_h} \right) p_{h_{tm}} - p_h(H_2O) \right] - y_m \left[\left(1 + \frac{V_t}{V_h} \right) p_{h_{tm}} - p_h \right]}{\eta V_w RT} \quad (4)$$

11 where y_f is the dry mole fraction of the air in the flask and y_m the mole fraction of the makeup
 12 gas = (543.9±0.3) ppb.

13 The extraction efficiency, η can be calculated from the following mass balance

14

$$15 \quad V_w c_{w0} = V_h c_h + \alpha V_w c_h \quad (5)$$

16 Assuming that headspace gas phase and water phase are in equilibrium, the ratio of the H_2
 17 concentration in water and in the headspace is given by the Ostwald coefficient (where the
 18 concentrations refer to in situ temperature):

19

$$20 \quad \alpha = \frac{c_w}{c_h} \quad (6)$$

21 This gives for the extraction efficiency as defined in equation (2)

22

$$23 \quad \eta = \left(1 + \alpha \frac{V_w}{V_h} \right)^{-1} \quad (7)$$

24 In the present case, $\alpha = \alpha(H_2)$ was equal to 0.0163±0.0001, which gives $\eta = 92.12 (\pm 0.013)\%$
 25 for $V_w/V_h = 8.4/1.6 = 5.25$.

26 Two alternative scenarios were considered to derive the δD of the dissolved H_2 , with scenario
 27 1 assuming equilibrium isotopic fractionation between headspace and water, and scenario 2
 assuming kinetic isotopic fractionation during extraction from Niskin bottle to glass vessel.

Scenario 1:

$$28 \quad \delta_{w0} = \delta_h + \varepsilon(1 - \eta)(1 + \delta_h) \quad (8)$$

Sylvia Walter 20.12.2015 21:33

$$y_f \left[\left(1 + \frac{V_t}{V_h} \right) p_{h_{tm}} - p_h \right]$$

Deleted: $c_{w0} = \frac{y_f \left[\left(1 + \frac{V_t}{V_h} \right) p_{h_{tm}} - p_h \right] - y_m \left[\left(1 + \frac{V_t}{V_h} \right) p_{h_{tm}} - p_h \right]}{\eta V_w RT}$ (4)

Sylvia Walter 20.12.2015 21:33
 Formatted: Text, Space After: 0 pt, Line spacing: 1.5 lines

Sylvia Walter 20.12.2015 21:33
 Formatted: Font:Not Italic

Sylvia Walter 20.12.2015 21:33
 Formatted: Left, Space After: 0 pt

Sylvia Walter 20.12.2015 21:33

Deleted: $V_w c_{w0} = V_h c_h + \alpha V_w c_h$

Sylvia Walter 20.12.2015 21:33

Deleted: $\alpha = \frac{c_w}{c_h}$

Sylvia Walter 20.12.2015 21:33
 Formatted: English (US)

Sylvia Walter 20.12.2015 21:33
 Formatted: Normal, Left

Sylvia Walter 20.12.2015 21:33

Deleted: $\eta = \left(1 + \alpha \frac{V_w}{V_h} \right)^{-1}$

Sylvia Walter 20.12.2015 21:33
 Formatted: Left, Space After: 0 pt

Sylvia Walter 20.12.2015 21:33
 Deleted: %

Sylvia Walter 20.12.2015 21:33
 Formatted: Left, Space After: 0 pt

Sylvia Walter 20.12.2015 21:33

Deleted: $\delta_{w0} = \delta_h + \varepsilon(1 - \eta)(1 + \delta_h)$

1 The equilibrium isotope fractionation between dissolved phase and gas phase is $\varepsilon = (37 \pm 1) \text{‰}$
2 at 20 °C [Knox *et al.*, 1992].

3 Scenario 2: $\delta_{w0} = \frac{(1+\delta_h)\eta}{1-(1-\eta)^{1+\varepsilon_k}} - 1 \approx \delta_h + \varepsilon_k(1-\eta)(1+\delta_h) \frac{\ln(1-\eta)}{\eta}$ (9)

4 The kinetic isotope fractionation during gas evasion is $\varepsilon_k = (-18 \pm 2) \text{‰}$ at 20 °C [Knox *et al.*,
5 1992]. The approximation is not used and only shown to illustrate the small difference
6 between δ_{w0} and δ_h when $\eta \approx 1$.

7 The temperature dependences of ε and ε_k are unknown and were neglected here.

8 The air saturation equilibrium concentration, $c_{\text{sat}}(\text{H}_2)$, was determined using the
9 parameterization of Wiesenburg and Guinasso (1979). The H_2 saturation anomaly, $\Delta(\text{H}_2)$, was
10 calculated as the difference between the measured H_2 concentration, $c(\text{H}_2)$, and $c_{\text{sat}}(\text{H}_2)$:

11 $\Delta(\text{H}_2) = c(\text{H}_2) - c_{\text{sat}}(\text{H}_2)$ (10)

12 Meteorological and oceanographic parameters (radiation, air and water temperatures, salinity,
13 relative humidity) were measured using standard instrumentation and recorded and provided
14 by the data system of the ships. More information about devices and sensor documentation
15 can be found on the website of the Alfred Wegener Institute <http://dship.awi.de/>. Backward
16 trajectories were calculated using the backward “Hybrid Single Particle Lagrangian Integrated
17 Trajectory” (HYSPLIT, Schlitzer 2012) model of the National Oceanic and Atmospheric
18 Administration (NOAA, <http://ready.arl.noaa.gov/HYSPLIT.php>).

19

20 2.5 Modeling

21 2.5.1 TM5 model

22 We performed simulations of H_2 mole fractions and isotopic composition with the global
23 chemistry transport model TM5 (Krol *et al.*, 2005), and compared them with our measurement
24 data (Fig. 5). The simulation setup was similar to the one of Pieterse *et al.* (2013) and only a
25 short description is given here. The model version used employs the full hydrogen isotopic
26 scheme from Pieterse *et al.* (2009) and uses ERA-Interim meteorological data. The chemistry
27 scheme is based on CBM-4 (Houweling *et al.*, 1998), which has been extended to include the
28 hydrogen isotopic scheme (that is, for all chemical species that include hydrogen atoms, HH
29 and HD are treated separately and have different reaction rates). The H_2 sources and isotopic
30 signatures are given as input; these and also the H_2 soil deposition velocities are identical to
31 Pieterse *et al.* (2013).

Sylvia Walter 20.12.2015 21:33

Deleted: $\delta_{w0} = \frac{(1+\delta_h)\eta}{1-(1-\eta)^{1+\varepsilon_k}} - 1 \approx \delta_h +$

Sylvia Walter 20.12.2015 21:33

Formatted: Left, Space After: 0 pt

Sylvia Walter 20.12.2015 21:33

Formatted: Font:Not Italic

Sylvia Walter 20.12.2015 21:33

Formatted: Left, Space After: 0 pt

Sylvia Walter 20.12.2015 21:33

Formatted: Font:Not Italic

Sylvia Walter 20.12.2015 21:33

Formatted: Font:Not Italic

1 The model has a relatively coarse spatial resolution of 6° longitude by 4° latitude, and a time
2 step of 45 minutes. Daily average mole fraction fields are used for comparison to
3 observations. The model results were interpolated to the time and location of the observations.

4

5 **2.5.2 Global oceanic emissions**

6 The climatological global oceanic emissions were calculated using the protocol of Pieterse et
7 al. (2013), based on the GEMS database and an assumed mean oceanic H_2 source of 5 Tg a^{-1}
8 as given from global budget calculations (see Ehhalt and Rohrer, 2009, and references therein,
9 Pieterse et al. 2013). The spatial and temporal variability of oceanic H_2 emissions caused by
10 N_2 fixation are adopted from the spatial and temporal distribution of oceanic CO (Erickson
11 and Taylor, 1992).

12

13 **3 Results and discussion**

14 **3.1 Atmospheric H_2 transects**

15 Our data set includes data of two hemispheres and two seasons between 2008 and 2010 (see
16 Table 2, Fig. 4). The mean mole fraction of H_2 ranged between (532.0 ± 10.7) ppb and
17 (548.5 ± 6.8) ppb. In spring, the mean values were almost equal between the hemispheres with
18 approximately 1 to 2 ppb difference, but they differed significantly in autumn. In this season,
19 the mean values in the northern hemisphere (NH) were approximately 16 ppb or 3 % lower
20 compared to the southern hemisphere (SH), with a distinct transition between the hemispheres
21 at around 8° N. In contrast, δD differed significantly between the hemispheres in both
22 seasons. In the southern hemisphere, absolute δD values were always between 9 and 27 ‰
23 higher than in the northern hemisphere, and generally remained within a narrow range
24 between (140.5 ± 21.1) ‰ and (145.4 ± 5.3) ‰. In contrast to the mole fraction, isotope delta
25 differences between the hemispheres were less pronounced in autumn than in spring. These
26 two seasonal patterns, in the following defined as “summer signal” and “winter signal”, are
27 mainly caused by biological processes and tropospheric photochemistry and driven by
28 variations in the NH. They are in line with previously published data and model results (Rhee
29 et al. 2006, Price et al. 2007, Rice et al. 2010, Pieterse et al. 2011, 2013, Batenburg et al.
30 2011, Yver et al. 2011, Yashiro et al. 2011).

1 The “summer signal”, observed in October, is characterized by lower H₂ mole fractions in the
2 northern hemisphere and a less pronounced difference in δD between the hemispheres.
3 Deposition by biological activity of microorganisms in the soils is the main sink of H₂
4 (Yonemura et al. 2000, Pieterse et al. 2013) and the sink strength in the northern and southern
5 hemisphere depends on the distribution of landmasses and on season. With approximately 70
6 % of landmasses in the NH and higher microbial activity in the summer, the mole fraction
7 during this season is lower in the NH than in the SH. Due to the general preference of
8 organisms for molecules with lighter isotopic composition, the δD values increase during
9 summer in the NH and the interhemispheric gradient becomes less pronounced.

10 The “winter signal” observed in April is defined by almost equal mole fractions and more
11 pronounced differences in δD values between the hemispheres. In winter, molecular hydrogen
12 is accumulating in the NH hemisphere, and the main source is fossil fuel combustion with a
13 depleted isotopic composition of -170 ‰ to -270 ‰ (Gerst and Quay, 2001; Rahn et al.,
14 2002). This leads to nearly equal mole fractions in both hemispheres and a more pronounced
15 δD gradient, with isotopically lighter H₂ in the NH. The contribution of source and sink
16 processes in the SH to the seasonal patterns is less pronounced than for the NH (Pieterse et al.
17 2011, 2013). As a result, the H₂ seasonal cycle in the SH is much weaker compared to the
18 NH. The SH isotopic H₂ signature is caused by mainly emissions and chemical loss with an
19 isotope delta of approximately $+190$ ‰, which explains the generally higher δD values. The
20 Intertropical Convergence Zone (ITCZ) separates the two hemispheres and is clearly visible,
21 not only in the H₂ distribution, but also in the CO distribution.

22 Simulations of H₂ mole fractions and isotopic composition using the global chemistry
23 transport model TM5 (Krol et al., 2005) compared with our atmospheric data reveal that the
24 model simulates the H₂ mole fractions quite well (Fig. 5), with a slight overestimate of up to
25 20 ppb (which means up to 4 %).

26 The model results are less variable on small spatial scales, due to the low spatial resolution,
27 and possibly to local influences that are not included in the model (e.g. ocean emissions in the
28 model are less variable in time and space than they could be in reality). The largest
29 differences between the modeled and measured H₂ occur between 30° S and the equator. This
30 seems a systematic feature and could be due to a slight overestimation of sources or
31 underestimation of sinks by the model. Despite these small differences, the model is
32 consistent with measured H₂ mole fractions and simulates them well. Large-scale features are

1 clearly visible, like the sharp gradient around 10° N during cruise ANT-XXVI/1 (Fig. 5, top,
2 third plot), or the decrease in δD towards northern mid-latitudes (most evident for the cruises
3 ANT-XXIV/4 and ANT-XXVI/4, first and last plots in Fig. 5, top). A slight overestimate of
4 the H₂ mole fractions was also noted by Pieterse et al. (2013). This might be explained by an
5 overestimate of photochemical sources in the model, which would influence only the mole
6 fractions but not the δD values.

7 The model simulates the isotopic composition of H₂ even better than the mole fractions. The
8 most important features are the general decrease from south to north, and the sharp gradient
9 around the equator. As most sources and sinks of H₂ have very different isotopic signatures,
10 this good comparison indicates that the model represents well both the magnitude and the
11 isotopic signature of the main components of the H₂ cycle. Similar to Pieterse et al. (2013) we
12 also observe a slight underestimate of the δD at high southern latitudes, which is possibly due
13 to underestimating the isotopic composition assumed for H₂ returning from the stratosphere in
14 the latitude band 60° S to 90° S.

15

16 **3.2 Spatial and temporal high-resolution transects during ANT-XXV/5**

17 In April 2009 the sampling resolution was increased to approximately one sample per two
18 hours for five selected sections of the transect during ANT-XXV/5 (Fig. 4, Table 3): three in
19 the southern hemisphere, one crossing the equator and one in the northern hemisphere. These
20 transects were chosen based on previously published data (Herr et al. 1984, Conrad and
21 Seiler, 1988) and with the aim to get an indication of small-scale sources or diurnal cycles of
22 atmospheric H₂ for further investigations.

23 All transects showed neither a diurnal cycle nor a correlation with radiation and a range of δD
24 values within or only slightly outside a 2 σ range around the mean, except for the one
25 between 23.5° S to 15.7° S (Fig. 6a). Here the highest H₂ mole fractions of (631.9±3.2) ppb,
26 combined with the lowest δD values of (20.9±5.0) ‰, were found around 16° S. Due to the
27 limited spatial resolution and therefore low number of data points a Keeling plot analysis
28 (Fig. 6b) of the data between 15° S and 18° S was made with either 5, 7, or 9 data points to
29 get a reasonable range for the source signature. It reveals a mean source signature of -561.5 in
30 a range of -530 ‰ to -683 ‰ ($n = 7 \pm 2$, $R^2 = 0.85 \pm 0.01$). The correlation coefficient is a
31 mean of the three analyses.

1 HYSPLIT trajectories for the samples collected on this transect during the 28 April 2010 and
2 1 May 2010 (21.8° S to 15.7° S) reveal the same origin of air masses coming from the
3 direction of Antarctica. Oceanographic parameters such as water temperature and salinity are
4 similar and do not correlate with H₂ mole fractions and δD values. These findings indicate a
5 strong but local source, and the low δD value for the source obtained by the Keeling plot
6 analysis points to biological production (Walter et al. 2012). Such local and temporal
7 patchiness of high H₂ mole fractions in surface waters was reported previously in correlation
8 to high N₂ fixation rates (Moore et al. 2009, 2014). Although reported for other oceanic
9 regions the H₂ mole fractions and δD values here do neither show a diurnal cycle (Herr et al.
10 1984) nor they are correlated with radiation indicating photochemical production (Walter et
11 al. 2013), and most of the values were observed during night. Wilson et al. (2013) recently
12 showed that H₂ production and uptake rates clearly depends on microbial species, and also on
13 their individual day–night rhythm, but the contribution of different diazotrophs to the marine
14 H₂ cycle is unknown (e.g. Bothe et al., 2010; Schütz et al., 2004; Wilson et al., 2010a and
15 2010b; Punshon and Moore, 2008b; Scranton 1983, Moore et al., 2009).

16 Around 21.2° S one single sample with a low mole fraction of (393.9±3.2) ppb in
17 combination with a high δD of (322.45±5) ‰ value was observed. As mentioned before
18 HYSPLIT models reveal the same origin of air masses on this transect, thus this sample
19 indicates probably a local sink. However, this interpretation depends on only one single
20 measurement point and although neither instrumental parameters indicated an outlier nor
21 meteorological or oceanographical parameters differed from other samples, we cannot
22 exclude an artefact due to sampling, storage, or analyses. A simple Rayleigh fractionation
23 model reveals a fractionation factor of $\alpha = 0.646 \pm 0.002$, which is close to the value of
24 oxidation by HO· ($\alpha = 0.58 \pm 0.07$, Batenburg et al. 2011). An estimate of the δD value by
25 using an HO· oxidation fractionation factor would lead to an increase by 125 ‰ or 149 ‰,
26 respectively. The observed increase of δD seems reasonable when assuming oxidation by
27 HO·, but with respect to the HO· mole fraction and the slow reaction rate of H₂ + HO· it is
28 questionable whether the H₂ decrease here can be explained by this.

29 **3.3 Dissolved H₂**

30 [A new method has been presented to extract H₂ from surface waters for isotopic](#)
31 [determination. Before discussing the measurement results, we will give an overview of the](#)

1 possible main errors and their effects. To show the effect of the errors on the measurements,
2 we will present error factors, thus how much the final data differ by shifting the respective
3 parameter by 1 % and also the absolute assumed error.

4 For the extraction method several error sources could be identified: the determination of
5 pressure, especially in the sampling vessel before adding the make-up gas and during
6 extraction, the temperature of air and water, respectively the difference between them when
7 the sample is extracted from the headspace, and the volume of the set-up and the sample. The
8 determination of pressure in the sampling vessel would be one issue of further improvement,
9 because the error caused by pressure deviations for the total pressure after adding the make-
10 up gas is about a factor of 0.7 for concentrations and 0.2 for the isotopic values. The error
11 based on temperature of air, water and sample is negligible due to high-precision
12 measurements and the short handling time between water sampling and headspace extraction.
13 The error for the volume parameter for the set-up is negligible due to the high volume, the
14 precise determination of the glass vessel volume by weighing, and the calculation of the
15 tubing volume. The main error source is the water volume of the sample, which counts by a
16 factor of 5.9 for the concentration, but with negligible effect on the isotopic values. Although
17 the relative error factor is quite high the absolute value is assumed to be around 0.5% due to
18 the sample size, which has also been weighed at the home lab. The H₂ measurement
19 procedure is the same as for atmospheric samples and possible errors are described in the
20 respective sessions or related literature. However, the error caused by the determination of the
21 dry mole fraction itself seems to have the main input by a factor of 5.3 for concentration and
22 4.6 for the isotopic values of dissolved H₂. Errors of the determination of the isotopic value
23 are much less significant and count by a factor of 0.2.

24 Taking measurement and handling errors during the extraction as well as errors in the
25 determination of the dry mole fraction into account, we assume a robust overall uncertainty of
26 $\pm 6.9\%$ for the dissolved H₂ mole fractions and $\pm 4.7\%$ for the isotopic values by calculating
27 the root of the sum of the squared uncertainties.

28 As shown in Table 4 we also tested the effect of equilibrium isotopic fractionation and kinetic
29 isotopic fractionation. The effect is less than 0.2%.

30 Therefore, recommendations for the extraction method are to additionally measure parameters
31 such as the initial pressure in the glass vessel and to ensure a precise determination of the

1 [sample volume. Besides this we recommend high-precision IRMS measurements and to](#)
2 [consider multiple sampling for better statistics on the data.](#)

4 3.3.1 H₂ concentration

5 In total 16 headspace samples were taken during the RV *Polarstern* cruise in April / May
6 2010 along the transect 32.53° W / 18.79° S to 13.00° W / 36.54° N and 6 samples during the
7 RV *L'Atalante* cruise in February 2008 between 23.00 – 17.93° W to 16.9 – 19.2° N to
8 analyse the H₂ mole fraction and the isotopic composition (see Table 4).

9 Although our setup was a prototype with possibilities for improvement, the mole fractions are
10 in line with previously published data. The H₂ excess, $\Delta(\text{H}_2)$, exceeds 5 nmol L⁻¹, the
11 saturation differ from close to equilibrium to 15-fold supersaturation. Highest supersaturation
12 was found in the southern hemisphere between 16° S and 11° S and in the northern
13 hemisphere around the Cape Verde islands and the coast of [Mauritania](#) (Fig. 7a, Table 4).

14 Herr et al. (1984) reported patchy enhanced H₂ concentrations in the surface water with up to
15 5-fold supersaturation in the subtropical south Atlantic (18 – 31° W and 29 – 42° W). This is
16 comparable to what Conrad and Seiler (1988) found in the Southern Atlantic, on a similar
17 cruise track as the RV *Polarstern*. Around the equator they measured H₂ surface water
18 concentrations up to 12-fold supersaturation. In the Southern Pacific, Moore et al. (2009)
19 combined H₂ surface water measurements with N₂ fixation measurements. They reported a
20 strong correlation between these parameters, a patchy distribution and a steep maximum of H₂
21 concentrations up to 12.6 nmol L⁻¹ around 14° S.

22 The recently published data by Moore et al. (2014) show similar patterns across the Atlantic
23 as we found, with highest values around the southern and northern subtropics. However, our
24 saturations are lower than the ones given by them, especially in the northern hemisphere.
25 Such differences might be caused by experimental issues such as overestimated extraction
26 efficiency or can be due to real temporal variability as the sampling seasons differed. The
27 extraction efficiency has been estimated as [92.12 \(±0.013\)%](#) (see Appendix) and was
28 incorporated into the calculation of the original seawater concentration. With respect to the
29 assumption of biological production as main production pathway it is more likely that due to
30 the different sampling seasons less H₂ was produced in April than in October / November
31 because of less microbial activity especially on the northern hemisphere in boreal winter.
32

Sylvia Walter 20.12.2015 21:33

Deleted: e.g. by adding a heat control or improved pressure monitoring

Sylvia Walter 20.12.2015 21:33

Deleted: Mauretania

Sylvia Walter 20.12.2015 21:33

Deleted: %

1 3.3.2 Isotopic composition of H₂

2 Additional information about H₂ sources comes from the analysis of the H₂ isotopic
3 composition. In the literature only one experimental value of dissolved marine δD exists, δD
4 = -628 ‰ (Price et al. 2007, Rice et al. 2010), but the origin of this value is unclear and it is
5 based on unpublished data. Nevertheless, this value has been used as representative for
6 oceanic emission in several global budget calculations (e.g. Price et al. 2007, Pieterse et al.
7 2011). Other authors (e.g. Rahn et al. 2003, Rhee et al. 2006) used a theoretical value of -700
8 ‰ , as expected for thermodynamic isotope equilibrium between H₂ and H₂O based on the
9 calculations of Bottinga (1969). The results presented here are the first well-documented
10 experimental results for isotope analysis of dissolved H₂ in seawater.

11 From the measurement of the isotopic composition of H₂ in the headspace we calculate the
12 isotopic composition of H₂ that was originally dissolved in the sea water as described in
13 section 2.4.3 and in the Appendix, using two different assumptions for fractionation between
14 dissolved H₂ and H₂ in the gas phase. The results shown in Table 4 reveal δD values for the
15 dissolved H₂ that vary within a wide range of -112 ‰ to -719 ‰ for both fractionation
16 scenarios. Interestingly, δD shows two distinct groups of samples that can be separated by the
17 water temperature (Fig. 7b). In water masses with a temperature above 21 °C the δD values
18 are $(-629 \pm 54) \text{ ‰}$ ($n = 14$), in water masses with a temperature of 20 °C or below δD values
19 are $(-249 \pm 88) \text{ ‰}$ ($n = 8$). There is no correlation of δD with salinity (Fig. 7c), but the high
20 temperature (and low δD) waters show also a generally higher saturation than the low
21 temperature (high δD) waters (Fig. 7d).

22 The very depleted isotope signature of the H₂ in the warmer water masses is consistent with
23 the values expected for biological production. The slight enrichment compared to the value of
24 $\approx -700 \text{ ‰}$ that is expected for biologically produced H₂ in equilibrium with ocean water
25 (Bottinga, 1969, Walter et al., 2012) may be caused by a partial consumption within the
26 water, which would enrich the remaining fraction. The relatively smooth distribution of the
27 isotopic composition of H₂ in the atmosphere strongly indicates that the contribution from
28 atmospheric variability cannot be a main contributor of the isotope variations observed in
29 dissolved H₂, even within the group of the depleted samples.

30 To our knowledge this is the first time that oceanic production of H₂ has been directly
31 attributed to biological processes by using isotope techniques. For the samples collected from
32 warm surface waters, our results verify the general assumption of a biological production

Sylvia Walter 20.12.2015 21:33

Deleted: have

Sylvia Walter 20.12.2015 21:33

Deleted: supersaturation

1 process as a main source of oceanic H₂ to the atmosphere rather than photochemical or other
2 sources (Herr et al. 1981, Conrad, 1988; Punshon and Moore, 2008, Moore et al. 2009). The
3 dominance of biological formation at higher temperatures is qualitatively consistent with the
4 general understanding of the temperature dependence of N₂ fixation rates for N₂ fixers such as
5 e.g. *Trichodesmium spec.*, which exhibit highest N₂ fixation rates within a temperature range
6 between 24 °C to 30 °C (Breitbarth et al. 2007, Stal 2009). In fact, the saturations also show a
7 correlation with temperature, but less clear than for δD (Fig. 7d), presumably due to
8 simultaneous uptake and consumption processes in a complex microbial community.
9 However, this clear attribution is only valid in water masses with higher temperatures and the
10 unexpectedly high δD values in cooler waters indicate the influence of other processes. The
11 isotopic enrichment that is expected for removal of H₂ (Chen et al., 2015, Rahn et al., 2003,
12 Constant et al., manuscript in preparation) is highly unlikely to cause a shift of almost 400 ‰
13 in δD from an assumed pure biological source, because in this case the removed fraction
14 would have to be unrealistically large, as also recently argued for soil emitted H₂ (Chen et al.,
15 2015). We suggest that a source of H₂ must exist in these surface waters, which produces H₂
16 that is out of isotope equilibrium with the water. This can be either one single source with an
17 isotopic signature of approximately -250 ‰, or an even more isotopically enriched source that
18 mixes with the depleted biological source.

19 Punshon and Moore (2008a, and references therein), reported abiotic photochemical H₂
20 production from CDOM and small organic compounds such as acetaldehyde or syringic acid.
21 Walter et al. (2013) indicated, that biologically active regions such as the Banc d'Arguin at
22 the coast of Mauritania could act as a pool of precursors such as VOCs for atmospheric H₂
23 with high δD values. It is thus possible that abiotic photochemical production in the surface
24 water might be an alternative source of H₂ excess, which is not isotopically equilibrated with
25 water, especially in regions with high radiation and biological activity, and less N₂ fixation.
26 Given the fact that the two groups of warm and cold waters are relatively well separated and
27 there is not a continuous mixing curve between two end members, the explanation of a single
28 different source seems more straightforward. Isotope analyses are a powerful tool to
29 distinguish this source from biological production. Additional measurements are needed to
30 determine the isotopic signature of such a source and investigate to which extent
31 photochemical production contributes to the oceanic H₂ budget in colder water masses, and
32 also update the current models. However, with an isotopic signature of approximately -250

1 %, or an even more isotopically enriched, such a source would not significantly impact the
2 current models.

3 Based on their H₂ measurements, Moore et al. (2014) suggested a substantial underestimation
4 of oceanic N₂ fixation, especially due to high H₂ supersaturations measured in the southern
5 hemisphere. By using direct measurements of N₂ fixation rates a systematic underestimation
6 by approximately 60 % was also proposed by Großkopf et al. (2012) who suggested a global
7 marine N₂ fixation rate of (177 ±8) Tg N a⁻¹. In order to identify a possible significant
8 mismatch between N₂ fixation rates and total marine H₂ production, we calculated the
9 climatological global oceanic emissions from the GEMS database using the protocol of
10 Pieterse et al. (2013), and an assumed mean oceanic H₂ source of 5 Tg a⁻¹ as given from
11 global budget calculations. The estimated emission rates and distributions in the Atlantic
12 Ocean (Fig. 8) are in line with the calculations of Moore et al. (2014), who reported H₂ sea-to-
13 air fluxes mostly in the range of (10±5) mmol m⁻² a⁻¹ and an almost equal distribution
14 between the hemispheres.

15 Westberry and Siegel (2006) estimated the global nitrogen fixation rate by *Trichodesmium*
16 blooms by using satellite ocean color data at 42 Tg N a⁻¹ and an additional 20 Tg N a⁻¹ under
17 non-bloom conditions, suggesting that *Trichodesmium* is likely the dominant organism in the
18 global ocean new nitrogen budget. The good agreement between our measurements of H₂
19 concentrations and δD and the model results from the TM5 model indicate that the oceanic
20 emissions of H₂ to the atmosphere are actually well represented in current atmospheric
21 models (Pieterse et al. 2013 and references herein). The proposed underestimate of oceanic N₂
22 fixation and a possible additional H₂ release during this process seems already be
23 incorporated in the current atmospheric budgets of H₂. Thus, supposing that both an assumed
24 total oceanic H₂ source of 5 Tg a⁻¹ to the atmosphere and a total global nitrogen fixation rate
25 of approximately 177 Tg N a⁻¹ are correct, our calculations clearly support the suggestion of
26 Großkopf et al. (2012) that N₂ fixers other than *Trichodesmium* have been severely
27 underestimated in the global picture and that the oceanic release ratio of H₂ to fixed N₂ clearly
28 needs more attention. Besides *Trichodesmium*, several other N₂-fixing organisms are known
29 for their potential to produce hydrogen (Wilson et al., 2010a; Falcón et al., 2002, 2004; Zehr
30 et al., 2001; Kars et al., 2009; Barz et al., 2010), and even non-N₂-fixing organisms might
31 play a role (Lilley et al. 1982).

32

Sylvia Walter 20.12.2015 21:33
Deleted: 175

1 **4 Conclusions**

2 Identifying sources is important to consider budgets and gain insight in production and
3 consumption processes. Although H₂ has been assumed reasonably to be produced mainly
4 biologically in the oceans, direct evidence was lacking. Our results verify a biological
5 production as a main source of H₂ in oceanic surface water, especially in warmer water
6 masses. As seen from the transects, local sources are difficult to spot due to their patchiness,
7 this should be taken into account when planning the sampling strategy.

8 The unexpectedly high δD values in colder temperate water masses indicate the significant
9 influence of processes other than biological production, and additional information e.g. by
10 isotopic composition is needed to distinguish and verify possible sources and supersaturations
11 of dissolved oceanic H₂. Especially the investigation of the isotopic composition of possible
12 production pathways such as abiotic photochemical H₂ production needs further attention and
13 should be an upcoming issue.

14 The pattern of mole fractions and isotopic composition of H₂ along a north–south Atlantic
15 transect clearly depends on season and hemisphere and are consistent with previous published
16 data and models. A possible significant underestimation of N₂ fixation as assumed by several
17 authors could – providing a net H₂ release rate – go along with higher H₂ emissions. However,
18 a comparison with the TM5 model and the calculation of the climatological global oceanic
19 emissions based on GEMS database reveal that the oceanic contribution to the global H₂
20 budget is reasonable and in general reproduced well and therefore a proposed underestimation
21 in the oceanic N₂ fixation seems already be corrected (from atmospheric considerations) in
22 the current atmospheric budgets of H₂. This also indicates, with respect to the proposed source
23 different than biological production in colder temperate water masses, that such a source
24 would probably not significantly impact the current models.

25 Besides the isotopic composition of photochemically produced H₂ the composition of N₂ fixer
26 communities and the release ratio of H₂ to N₂ fixed needs more investigation to understand
27 the general processes and distributions of oceanic H₂ in more detail.

28

29 **Acknowledgements**

30 We are very thankful to the crew of the RV *Polarstern* and RV *L'Atalante* for their friendly
31 and professional help and support. This study was financed by the NWO (Netherlands
32 Organization for Scientific Research), NWO project number 816.01.001, the EU FP7 project

1 InGOS (GA number 284274), and the BMBF (Bundesministerium für Bildung und
2 Forschung) project SOPRAN, grant FKZ 03F0462, grant 03F0611 and grant 03F0662.
3

1 References

- 2 Barz, M., Beimgraben, C., Staller, T., Germer, F., Opitz, F., Marquardt, C., Schwarz, C.,
3 Gutekunst, K., Vanselow, K.H., Schmitz, R., LaRoche, J., Schulz, R., and Appel, J.:
4 Distribution analysis of hydrogenases in surface waters of marine and freshwater
5 environments, *PLoS ONE*, 5(11), e13846, doi:10.1371/journal.pone.0013846, 2010.
- 6 Batenburg, A. M., Walter, S., Pieterse, G., Levin, I., Schmidt, M., Jordan, A., Hammer, S.,
7 Yver, C., and Röckmann, T.: Temporal and spatial variability of the stable isotopic
8 composition of atmospheric molecular hydrogen: observations at six EUROHYDROS
9 stations, *Atmos. Chem. Phys.*, 11, 6985–6999, doi:10.5194/acp-11-6985-2011, 2011.
- 10 [Battino, R.: The Ostwald coefficient of gas solubility, *Fluid Phase Equilib.*, 15, 231-240,](#)
11 [13003–13021](http://dx.doi.org/10.1016/0378-3812(84)87009-0, 1984</p><p>12 Bothe, H., Neuer, G., Kalbe, I., and Eisbrenner, G.: Electron donors and hydrogenase in
13 nitrogen-fixing microorganisms, in: Stewart WDP, Gallon JR (eds) <i>Nitrogen fixation</i>.
14 Academic Press, London, p 83–112, 1980.</p><p>15 Bothe, H., Schmitz, O., Yates, M. G., and Newton, W. E.: Nitrogen fixation and hydrogen
16 metabolism in cyanobacteria, <i>MMBR</i>, 74(4), 529–51, doi:10.1128/MMBR.00033-10, 2010.</p><p>17 Breitbart, E., Oschlies, A., and LaRoche, J.: Physiological constraints on the global
18 distribution of <i>Trichodesmium</i> – effect of temperature on diazotrophy, <i>Biogeosciences</i>, 4, 53–
19 61, 2007.</p><p>20 Bottinga, Y.: Calculated fractionation factors for carbon and hydrogen isotope exchange in
21 the system calcite–carbon dioxide–graphite–methane–hydrogen–water vapour, <i>Geochim.</i>
22 <i>Cosmochim. Ac.</i>, 33, 49–64, 1969.</p><p>23 Chen, Q., Popa, E.M., Batenburg, A.M., and Röckmann, T.: Isotopic signatures of production
24 and uptake of H₂ by soil, <i>Atmos. Chem. Phys.</i>, 15, <a href=), doi:10.5194/acp-15-13003-
25 2015, 2015
- 26 Conrad, R., and Seiler, W.: Methane and hydrogen in seawater (Atlantic Ocean), *Deep-Sea*
27 *Res.*, 35(12), 1903–1917, 1988.
- 28 Constant, P., Walter, S., Batenburg, A.M., Liot, Q.; and Röckmann, T.: Kinetics and isotopic
29 signature of the H₂ uptake activity of three Actinobacteria scavenging atmospheric H₂, in
30 preparation, 2015
- 31 Ehhalt, D.H., and Rohrer, F.: The tropospheric cycle of H₂: a critical review, *Tellus B*, 61,
32 500–535, 2009.

Sylvia Walter 20.12.2015 21:33

Deleted:

Sylvia Walter 20.12.2015 21:33

Deleted: Discuss

Sylvia Walter 20.12.2015 21:33

Deleted: 23457-23506

Sylvia Walter 20.12.2015 21:33

Deleted: acpd

Sylvia Walter 20.12.2015 21:33

Deleted: 23457

1 Erickson, D. J., and Taylor, J. A.: 3-D Tropospheric CO modeling: The possible influence of
2 the ocean, *Geophys. Res. Lett.*, 19, 1955–1958, 1992

3 Falcón, L.I., Cipriano, F., Chistoserdov, A.Y., and Carpenter, E.J.: Diversity of diazotrophic
4 unicellular cyanobacteria in the tropical North Atlantic Ocean, *Appl. Environ. Microbiol.*,
5 68(11), 5760–5764, doi:10.1128/AEM.68.11.5760.2002, 2002.

6 Falcón, L.I., Carpenter, E.J., Cipriano, F., Bergman, B., and Capone, D.G.: N₂ fixation by
7 unicellular bacterioplankton from the Atlantic and Pacific Oceans: Phylogeny and in situ
8 rates, *Appl. Environ. Microbiol.*, 70(2), 765–770, doi:10.1128/AEM.70.2.765–770.2004,
9 2004.

10 Feck, T., Groß, J.-U., and Riese, M.: Sensitivity of Arctic ozone loss to stratospheric H₂O,
11 *Geophys. Res. Lett.*, 35, L01803, doi:10.1029/2007GL031334, 2008.

12 Feilberg, K.L., Johnson, M.S., Bacak, A., Röckmann, T., and Nielsen, C.J.: Relative
13 tropospheric photolysis rates of HCHO and HCDO measured at the European photoreactor
14 facility, *J. Phys. Chem. A*, 111(37), 9034–9046, 2007.

15 Gerst, S., and Quay, P.: Deuterium component of the global molecular hydrogen cycle, *J.*
16 *Geophys. Res.*, 106, 5021–5031, 2001.

17 [Green, E.J., and Carritt, D.E.: New tables for oxygen saturation of seawater, *J. Mar. Res.*, 25,](#)
18 [140-147, 1967](#)

19 Großkopf, T., Mohr, W., Baustian, T., Schunck, H., Gill, D., Kuypers, M.M.M., Lavik, G.,
20 Schmitz, R.A., Wallace, D.W.R., LaRoche, J.: Doubling of marine dinitrogen-fixation rates
21 based on direct measurements, *Nature*, 488, 361–364, doi:10.1038/nature11338, 2012.

22 Hanschmann, T., Deneke, H., Roebeling, R., and Macke, A.: Evaluation of the shortwave
23 cloud radiative effect over the ocean by use of ship and satellite observations, *Atmos. Chem.*
24 *Phys.*, 12, 12243–12253, doi:10.5194/acp-12-12243-2012, 2012.

25 Hauglustaine, D.A., and Ehhalt, D.H.: A three-dimensional model of molecular hydrogen in
26 the troposphere, *J. Geophys. Res.*, 107(D17), 4330–4346, doi:10.1029/2001JD001156, 2002.

27 Herr, F.L.: Dissolved hydrogen in Eurasian Arctic waters, *Tellus*, 36B, 55–66, 1984.

28 Herr, F.L., Scranton, M.I., and Barger, W.R.: Dissolved hydrogen in the Norwegian Sea:
29 Mesoscale surface variability and deep-water distribution, *Deep-Sea Res.*, 28A(9), 1001–
30 1016, 1981.

31 Herr, F.L., Frank, E.C., Leone, G.M., and Kennicutt, M.C.: Diurnal variability of dissolved
32 molecular hydrogen in the tropical South Atlantic Ocean, *Deep-Sea Res.*, 31(1), 13–20, 1984.

1 Houweling, S., Dentener, F., and Lelieveld, J.: The impact of non-methane hydrocarbon
2 compounds on tropospheric photochemistry, *J. Geophys. Res.*, 103(D9), 10673–10696,
3 doi:10.1029/97JD03582, 1998.

4 Jacobson, M.Z., Colella, W.G., and Golden, D.M.: Cleaning the air and improving health with
5 hydrogen fuel-cell vehicles, *Science*, 308, 1901–1905, 2005.

6 Jacobson, M.Z.: Effects of wind-powered hydrogen fuel cell vehicles on stratospheric ozone
7 and global climate, *Geophys. Res. Lett.*, 35, L19803, doi:10.1029/2008GL035102, 2008.

8 Jordan, A. and Steinberg, B.: Calibration of atmospheric hydrogen measurements, *Atmos.*
9 *Meas. Tech.*, 4, 509–521, doi:10.5194/amt-4-509-2011, 2011.

10 Kars, G., Gündüz, U., Yücel, M., Rakhely, G., Kovacs, K.L., & Eroğlu, İ.: Evaluation of
11 hydrogen production by *Rhodobacter sphaeroides* O.U.001 and its *hupSL* deficient mutant
12 using acetate and malate as carbon sources. *Int. J. Hydrogen Energ.*, 34(5), 2184–2190.
13 Doi:10.1016/j.ijhydene.2009.01.016, 2009.

14 Knox, M., Quay, P.D., and Wilbur, D.: Kinetic isotopic fractionation during air-water gas
15 transfer of O₂, N₂, CH₄, and H₂, *J. Geophys. Res.*, 97(C12), 20335–20343, 1992.

16 Kock, A., Gebhardt S., and Bange, H.W.: Methane emissions from the upwelling area off
17 Mauritania (NW Africa), *Biogeosciences*, 5, 1119–1125, doi:10.5194/bg-5-1119-2008, 2008.

18 Krol, M., Houweling, S., Bregman, B., van den Broek, M., Segers, A., van Velthoven, P.,
19 Peters, W., Dentener, F., and Bergamaschi, P.: The two-way nested global chemistry-
20 transport zoom model TM5: Algorithm and applications, *Atmos. Chem. Phys.*, 5(2), 417–432,
21 doi:10.5194/acp-5-417-2005, 2005.

22 Lilley, M.D., Baross, J.A., and Gordon, L.I.: Dissolved hydrogen and methane in Saanich
23 Inlet, British Columbia, *Deep-Sea Res.*, 29(12A), 1471–1484, 0198–0149/82/121471–13,
24 Printed in Great Britain, Pergamon Press Ltd., 1982.

25 Longhurst, A.R.: *Ecological Geography of the Sea*, 398 pp., Academic, San Diego,
26 California, 1998.

27 Moore, R.M., Punshon, S., Mahaffey, C., and Karl, D.: The relationship between dissolved
28 hydrogen and nitrogen fixation in ocean waters, *Deep-Sea Res.*, 56, 1449–1458,
29 doi:10.1016/j.dsr.2009.04.008, 2009.

30 Moore, R.M., Kienast, M., Fraser, M., Cullen, J.J., Deutsch, C., Dutkiewicz, S., Follows, M.
31 J., and Somes, C.J.: Extensive hydrogen supersaturations in the western South Atlantic Ocean
32 suggest substantial underestimation of nitrogen fixation, *J. Geophys. Res. Oceans*, 119, 4340–

Sylvia Walter 20.12.2015 21:33

Formatted: Font:12 pt

Sylvia Walter 20.12.2015 21:33

Formatted: Font:12 pt

Sylvia Walter 20.12.2015 21:33

Formatted: Font:12 pt

Sylvia Walter 20.12.2015 21:33

Formatted: Font:Myriad Hebrew Italic

1 4350, doi:10.1002/2014JC010017, 2014.

2 Nilsson, E., Johnson, M.S., Taketani, F., Matsumi, Y., Hurley, M.D., and Wallington, T.J.:
3 Atmospheric deuterium fractionation: HCHO and HCDO yields in the CH₂DO + O₂ reaction,
4 *Atmos. Chem. Phys.*, 7, 5873–5881, 2007.

5 Nilsson, E.J.K., Andersen, V.F., Skov, H., and Johnson, M.S.: Pressure dependence of the
6 deuterium isotope effect in the photolysis of formaldehyde by ultraviolet light, *Atmos. Chem.*
7 *Phys.*, 10, 3455–3463, 2010.

8 Novelli, P.C., Lang, P.M., Masarie, K.A., Hurst, D.F., Myers, R., and Elkins, J.W.: Molecular
9 hydrogen in the troposphere: Global distribution and budget, *J. Geophys. Res.*, 104, 30427–
10 30444, 1999.

11 Pieterse, G., Krol, M.C., and Röckmann, T.: A consistent molecular hydrogen isotope
12 chemistry scheme based on an independent bond approximation, *Atmos. Chem. Phys.*, 9,
13 8503–8529, 2009.

14 Pieterse, G., Krol, M.C., Batenburg, A.M., Steele, L.P., Krummel, P.B., Langenfelds, R.L.,
15 and Röckmann, T.: Global modelling of H₂ mixing ratios and isotopic compositions with the
16 TM5 model, *Atmos. Chem. Phys.*, 11(14), 7001–7026, doi:10.5194/acp-11-7001-2011, 2011.

17 Pieterse, G., Krol, M.C., Batenburg, A.M., Brenninkmeijer, C.A.M., Popa, M.E., O’Doherty,
18 S., Grant, A., Steele, L.P., Krummel, P.B., Langenfelds, R.L., Wang, H.J., Vermeulen, A.T.,
19 Schmidt, M., Yver, C., Jordan, A., Engel, A., Fisher, R.E., Lowry, D., Nisbet, E.G., Reimann,
20 S., Vollmer, M.K., Steinbacher, M., Hammer, S., Forster, G., Sturges, W.T., and Röckmann,
21 T.: Reassessing the variability in atmospheric H₂ using the two-way nested TM5 model, *J.*
22 *Geophys. Res. Atmos.*, 118, 3764–3780, doi:10.1002/jgrd.50204, 2013.

23 Popa, M.E., Vollmer, M.K., Jordan, A., Brand, W.A., Pathirana, S.L., Rothe, M., Röckmann,
24 T.: Vehicle emissions of greenhouse gases and related tracers from a tunnel study: CO:CO₂,
25 N₂N₂O:CO₂, CH₄:CO₂, O₂:CO₂ ratios, and the stable isotopes ¹³C and ¹⁸O in CO₂ and CO,
26 *Atmos. Chem. Phys.*, 14, 2105–2123, doi:10.5194/acp-14-2105-2014, 2014.

27 Popa, M.E., Segers, A.J., van der Gon, H.A.C.D., Krol, M.C., Visschedijk, A.J.H., Schaap,
28 M., and Rockmann, T.: Impact of a future H₂ transportation on atmospheric pollution in
29 Europe, *Atmos Environ.*, 113, 208–222, doi:10.1016/j.atmosenv.2015.03.022, 2015.

30 Prather, M.J.: An environmental experiment with H₂?, *Science*, 302, 581–582, 2003.

31 Price, H., Jaegle, L., Rice, A., Quay, P., Novelli, P.C., Gammon, R.: Global budget of
32 molecular hydrogen and its deuterium content: constraints from ground station, cruise, and

1 aircraft observations, *J. Geophys. Res.*, 112, D22108, doi:10.1029/2006JD008152, 2007.

2 Punshon, S., Moore, R.M., and Xie, H.: Net loss rates and distribution of molecular hydrogen
3 (H_2) in mid-latitude coastal waters, *Mar. Chem.*, 105(1–2), 129–139,
4 doi:10.1016/j.marchem.2007.01.009, 2007.

5 Punshon, S., and Moore, R.: Photochemical production of molecular hydrogen in lake water
6 and coastal seawater, *Mar. Chem.*, 108(3–4), 215–220, doi:10.1016/j.marchem.2007.11.010,
7 2008a.

8 Punshon, S., and Moore, R.M.: Aerobic hydrogen production and dinitrogen fixation in the
9 marine cyanobacterium *Trichodesmium erythraeum* IMS101, *Limnol. Oceanogr.*, 53(6),
10 2749–2753, 2008b.

11 Rahn, T., Kitchen, N., and Eiler, J.M.: D/H ratios of atmospheric H_2 in urban air: Results
12 using new methods for analysis of nano-molar H_2 samples, *Geochim. Cosmochim. Acta*, 66,
13 2475–2481, 2002.

14 Rahn, T., Eiler, J.M., Boering, K.A., Wennberg, P.O., McCarthy, M.C., Tyler, S., Schauffler,
15 S., Donnelly, S., and Atlas, E.: Extreme deuterium enrichment in stratospheric hydrogen and
16 the global atmospheric budget of H_2 , *Nature*, 424, 918–921, 2003.

17 Rhee, T.S., Mak, J., Röckmann, T., and Brenninkmeijer, C.A.M.: Continuous-flow isotope
18 analysis of the deuterium/hydrogen ratio in atmospheric hydrogen, *Rapid Commun. Mass*
19 *Spectrom.*, 18 (3), 299–306, doi: 10.1002/rcm.1309, 2004.

20 Rhee, T.S., Brenninkmeijer, C.A.M., and Röckmann, T.: The overwhelming role of soils in
21 the global atmospheric hydrogen cycle, *Atmos. Chem. Phys.*, 6, 1611–1625, 2006.

22 Rice, A., Quay, P., Stutsman, J., Gammon, R., Price, H., and Jaegle, L.: Meridional
23 distribution of molecular hydrogen and its deuterium content in the atmosphere, *J. Geophys.*
24 *Res.*, 115, D12306, doi:10.1029/2009JD012529, 2010.

25 Robinson, C., Holligan, P., Jickels, T., and Lavender, S.: The Atlantic Meridional Transect
26 Programme (1995 – 2012), *Deep-Sea Res. II*, 56, 895–898, doi:10.1016/j.dsr2.2008.10.005,
27 2009.

28 Röckmann, T., Rhee, T.S., and Engel, A.: Heavy hydrogen in the stratosphere, *Atmos. Chem.*
29 *Phys.*, 3, 2015–2023, 2003.

30 Röckmann, T., Gómez Álvarez, C.X., Walter, S., van Veen, C., Wollny, A.G., Gunthe, S.S.,
31 Helas, G., Pöschl, U., Keppler, F., Greule, M., and Brand, W.A.: The isotopic composition of

1 H₂ from wood burning – dependency on combustion efficiency, moisture content and δD of
2 local precipitation, *J. Geophys. Res.*, 115, D17308, doi:10.1029/2009JD013188, 2010a.

3 Röckmann, T., Walter, S., Bohn, B., Wegener, R., Spahn, H., Brauers, T., Tillmann, R.,
4 Schlosser, E., Koppmann, R., and Rohrer, F.: Isotope effect in the formation of H₂ from
5 H₂CO studied at the atmospheric simulation chamber SAPHIR, *Atmos. Chem. Phys.*, 10,
6 5343–5357, 2010b.

7 Schlitzer, R., *Ocean Data View* 4, <http://odv.awi.de>, 2012.

8 Schultz, M.G., Diehl, T., Brasseur, G.P., and Zittel, W.: Air pollution and climate–forcing
9 impacts of a global hydrogen economy, *Science*, 302, 624–627, 2003.

10 Schütz, K., Happe, T., Troshina, O., Lindblad, P., Leitão, E., Oliveira, P., and Tamagnini, P.:
11 Cyanobacterial H₂ production – a comparative analysis, *Planta*, 218(3), 350–359,
12 doi:10.1007/s00425–003–1113–5, 2004.

13 Scranton, M., Jones, M., and Herr, F.L.: Distribution and variability of hydrogen in the
14 Mediterranean Sea, *J. Mar. Res.* 40: 873–891, 1982.

15 Scranton, M.I.: The role of the cyanobacterium *Oscillatoria (Trichodesmium) thiebautii* in the
16 marine hydrogen cycle, *Mar. Ecol.*, 11(1), 79–87, 1983.

17 Seiler, W., and Schmidt, U.: Dissolved non–conservative gases in seawater. In: Goldberg ED
18 (ed) *The sea*, Vol 5. John Wiley & Sons, New York, p 219–243, 1974.

19 Stal, L.J.: Is the distribution of nitrogen–fixing cyanobacteria in the oceans related to
20 temperature?, *Environmental Microbiology*, 11(7), 1632–1645, doi:10.1111/j.1758–
21 2229.2009.00016.x, 2009.

22 Tamagnini, P., Leitão, E., Oliveira, P., Ferreira, D., Pinto, F., Harris, D. J., Heidorn, T., and
23 Lindblad, P.: Cyanobacterial hydrogenases: diversity, regulation and applications, *FEMS*
24 *microbiology reviews*, 31(6), 692–720, doi:10.1111/j.1574–6976.2007.00085.x, 2007.

25 Tromp, T.K., Shia, R.-L., Allen, M., Eiler, J.M., and Yung, Y.L.: Potential environmental
26 impact of a hydrogen economy on the stratosphere, *Science*, 300, 1740–1742, 2003.

27 Vollmer, M.K., Walter, S., Bond, S.W., Soltic, P., and Röckmann, T.: Molecular hydrogen
28 (H₂) emissions and their isotopic signatures (H/D) from a motor vehicle: implications on
29 atmospheric H₂, *Atmos. Chem. Phys.*, 10, 5707–5718, doi:10.5194/acp–10–5707–2010, 2010.

30 Walter, S., Laukenmann, S., Stams, A.J.M., Vollmer, M.K., Gleixner, G., and Röckmann, T.:
31 The stable isotopic signature of biologically produced molecular hydrogen (H₂),
32 *Biogeosciences* 9, 4115–4123, doi:10.5194/bg–9–4115–2012, 2012.

1 Walter, S., Kock, A., and Röckmann, T.: High-resolution measurements of atmospheric
2 molecular hydrogen and its isotopic composition at the West African coast of Mauritania,
3 Biogeosciences, 10, 3391–3403, doi:10.5194/bg-10-3391-2013, 2013.

4 Warwick, N.J., Bekki, S., Nisbet, E.G., and Pyle, J.A.: Impact of a hydrogen economy on the
5 stratosphere and troposphere studied in a 2-D model, Geophys. Res. Lett., 31, L05107,
6 doi:10.1029/2003GL019224, 2004.

7 Westberry, T.K., and Siegel, D.A.: Spatial and temporal distribution of *Trichodesmium*
8 blooms in the world's oceans, Global Biogeochem. Cycles, 20, GB4016,
9 doi:10.1029/2005GB002673, 2006.

10 Wiesenburg, D.A., and Guinasso, N.L.: Equilibrium solubilities of methane, carbon
11 monoxide, and hydrogen in water and sea water, J. Chem. Eng. Data, 1979, 24 (4), pp 356–
12 360, doi:10.1021/je60083a006, 1979.

13 Wilson, S.T., Foster, R.A., Zehr, J.P., and Karl, D.M.: Hydrogen production by
14 *Trichodesmium erythraeum*, *Cyanothece* sp., and *Crocospaera watsonii*, Aquat. Microb.
15 Ecol., 59(2), 197–206, doi:10.3354/ame01407, 2010a.

16 Wilson, S.T., Tozzi, S., Foster, R.A., Ilikchyan, I., Kolber, Z.S., Zehr, J.P., and Karl, D.M.:
17 Hydrogen cycling by the unicellular marine diazotrophs *Crocospaera watsonii* strain
18 WH8501, Appl. Environ. Microb., 76(20), 6797–803, doi:10.1128/AEM.01202-10, 2010b.

19 Wilson, S.T., del Valle, D.A., Robidart, J.C., Zehr, J.P., and Karl, D.M.: Dissolved hydrogen
20 and nitrogen fixation in the oligotrophic North Pacific Subtropical Gyre, Environ. Microbiol.
21 Rep., 5(5), 697–704, doi: 10.1111/1758-2229.12069, 2013.

22 Yashiro, H., Sudo, K., Yonemura, S., and Takigawa, M.: The impact of soil uptake on the
23 global distribution of molecular hydrogen: chemical transport model simulation, Atmos.
24 Chem. Phys., 11, 6701–6719, doi:10.5194/acp-11-6701-2011, 2011.

25 Yonemura, S., Kawashima, S., and Tsuruta, H.: Carbon monoxide, hydrogen, and methane
26 uptake by soils in a temperate arable field and a forest, J. Geophys. Res. 105, 14347–14362,
27 DOI: 10.1029/1999JD901156, 2000.

28 Yver, C.E., Pison, I.C., Fortems-Cheiney, A., Schmidt, M., Chevallier, F., Ramonet, M.,
29 Jordan, A., Søvde, O.A., Engel, A., Fisher, R.E., Lowry, D., Nisbet, E.G., Levin, I., Hammer,
30 S., Necki, J., Bartyzel, J., Reimann, S., Vollmer, M.K., Steinbacher, M., Aalto, T., Maione,
31 M., Arduini, J., O'Doherty, S., Grant, A., Sturges, W.T., Forster, G.L., Lunder, C.R.,
32 Privalov, V., Paramonova, N., Werner, A., and Bousquet, P.: A new estimation of the recent

1 tropospheric molecular hydrogen budget using atmospheric observations and variational
2 inversion, *Atmos. Chem. Phys.*, 11, 3375–3392, doi:10.5194/acp-11-3375-2011, 2011.
3 Zehr, J.P., Waterbury, J.B., Turner, P.J., Montoya, J.P., Omoregie, E., Steward, G.F., Hansen,
4 A., Karl, D.M.: Unicellular cyanobacteria fix N₂ in the subtropical North Pacific Ocean.
5 *Nature*, 412(6847), 635–638, 2001.

6

7

1
2
3
4

Table 1: Overview of sample distribution during the cruises: type A are discrete atmospheric samples, type H are headspace samples extracted from the surface water. The sample numbers in brackets give the number of measured samples in the northern (NH) and southern (SH) hemisphere.

Cruise	Date	Position (start – end)	Nr. of Samples (NH / SH)	Type
ANT-XXIV/4	18.04. – 20.05.2008	59.15 °W / 46.13 ° S – 06.21 °W / 47.96 °N	95 (44 NH / 51 SH)	A
ANT-XXV/5	11.04. – 24.05.2009	50.99 °W / 40.82 ° S – 23.05 °W / 16.55 °N	91 (30 NH / 61 SH)	A
ANT XXVI/1	16.10. – 25.11.2009	12.05 °W / 37.96 °N – 47.28 °W / 37.43 ° S	60 (29 NH / 31 SH)	A
ANT XXVI/4	07.04. – 17.05.2010	58.14 °W / 43.75 ° S – 04.46 °E / 53.15 °N	114 (56 NH / 58 SH)	A
ANT XXVI/4	07.04. – 17.05.2010	32.53 °W / 18.79 ° S – 13.00 °W / 36.54 °N	16 (10 NH / 6 SH)	H
L'Atalante ATA-3	03.02. – 20.02.2008	17.83 °N / 16.56 °W – 17.60 °N / 24.24 °W	6 (6N H / 0 SH)	H

5
6
7
8

1 Table 2: Hemispheric means of atmospheric H₂ and its isotopic composition along the four meridional Atlantic transects

Cruise	Southern Hemisphere				Northern Hemisphere			
	IRMS – H ₂ mole fraction [ppb]	δD [‰]	RGA – H ₂ mole fraction [ppb]	RGA – CO mole fraction [ppb]	IRMS – H ₂ mole fraction [ppb]	δD [‰]	RGA – H ₂ mole fraction [ppb]	RGA – CO mole fraction [ppb]
ANT-XXI/4 April 2008	mean 543.4±7.3 range 528.8 – 568.5 n 49 (2 values excluded)	145.4±5.3 135.4 – 155.7 49 (2 values excluded)	No data	No data	544.1±9.8 522.0 – 567.8 44	118.6±3.9 110.4 – 130.9 44	No data	No data
ANT-XXV/5 April 2009	mean 533.9±38.7 range 350.2 – 631.9 n 60	140.5±21.1 20.9 – 166.1 60	520.4±24.0 432.5 – 545.1 21	59.9±17.7 43.6 – 119.6 21	532.94±19.73 466.9 – 560.3 28 (2 values excluded)	121.28±7.09 89.1 – 130.9 28 (2 values excluded)	526.18±12.6 508.9 – 564.1 29	112.67±21.3 76.9 – 190.5 29
ANT-XXVI/1 October 2009	mean 548.5±6.8 range 535.9 – 563.4 n 30 (1 value excluded)	143.2±4.2 135.5 – 149.3 30 (1 value excluded)	546.4±7.4 531.4 – 563.0 49	59.9±10.5 47.7 – 85.8 49	532.04±10.65 501.1 – 551.7 29	133.94±4.43 123.5 – 141.7 29	526.02±10.53 494.2 – 548.8 46	76.73±7.43 65.4 – 96.1 46
ANT-XXVI/4 April 2010	mean 541.6±16.3 range 496.0 – 579.6 n 58	143.7±11.5 89.3 – 161.8 58	525.1±29.1 481.5 – 696.8 617	47.2±8.8 36.2 – 121.8 617	539.4±14.8 505.5 – 564.6 56	116.2±11.5 93.8 – 146.6 56	507.8±15.7 481.3 – 603.8 1339	120.8±11.2 72.7 – 146.1 1339

2
3
4
5
6
7
8
9

1 Table 3: Overview of means of atmospheric H₂ and its isotopic composition along the five high-resolution transects of ANT-XXV/5,
 2 including the standard deviation and the range

Transect (latitude)		Mole fraction [ppb]	δD [‰]
40.8° S / 38.9° S n = 12	mean	515.5±37.7	141.4±6.2
	range	448.4 – 566.9	129.3 – 151.0
33.0° S / 30.8° S n = 12	mean	521.4±53.3	152.9±5.9
	range	350.2 – 551.9	142.8 – 166.1
23.5° S / 15.7° S n = 32	mean	536.9±38.4	144.1±41.4
	range	392.9 – 631.9	20.91 – 322.45
2.0° S / 3.2° N n = 11	mean	537.5±36.2	119.5±12.6
	range	466.9 – 592.2	89.1 – 135.5
9.9° N / 16.2° N n = 21	mean	537.0±12.2	122.5±3.0
	range	511.0 – 560.3	118.4 – 131.0

3
4

1 Table 4: overview of headspace sample results from the ANT-XXVI/4 cruise (2010) and the L'Atalante ATA-3 (2008). γ_a is the measured
 2 mole fraction of the headspace in parts per billion (ppb = nmole mole⁻¹), γ_a is the corresponding atmospheric mole fraction in ppb, δD_n and
 3 δD_n is the measured isotopic composition in permill [‰]. The H₂ equilibrium concentration $c_{sat}(H_2)$ was determined by using the equations
 4 from Wiesenburg and Guinasso (1979), the initial dissolved H₂ concentration c_{w0} is calculated as given in Appendix 1, and the excess ΔH_2 is
 5 the difference between them. $\delta_{w0\ SC1}$ and $\delta_{w0\ SC2}$ show the two scenarios to derive the initial isotope delta of dissolved H₂. $S_{(H_2)}$ is the
 6 saturation of H₂ in the surface water. The calculated extraction efficiency was 92.12 (±0.13)%. The calculations are given in the Appendix
 7 in more detail.

Date / Time [UTC]	Sampling position	γ_a [ppb]	δD_n [‰]	γ_e [ppb]	δD_n [‰]	$c_{sat}(H_2)$ [nmol L ⁻¹]	c_{w0} [nmol L ⁻¹]	$\Delta(H_2)$ [nmol L ⁻¹]	$\delta_{w0\ SC1}$ [‰]	$\delta_{w0\ SC2}$ [‰]	$S_{(H_2)}$ [%]
21.04.2010 15:15	-18.79 °N -32.53 °E	562.0	148.5	653.3	-37.3	0.35	1.68	1.32	-536.2	-535.6	↓75
22.04.2010 15:24	-15.91 °N -30.49 °E	524.2	134.5	750.6	-138.6	0.33	2.89	2.57	-654.8	-654.4	↓80
23.04.2010 15:21	-13.06 °N -28.51 °E	551.6	144.3	754.4	-125.1	0.35	2.91	3.57	-602.9	-602.5	↓41
24.04.2010 15:36	-10.71 °N -26.92 °E	522.0	153.2	797.0	-151.2	0.33	3.52	3.19	-605.6	-605.2	↓074
25.04.2010 15:24	-7.97 °N -25.02 °E	542.9	154.7	674.8	-59.4	0.34	1.97	1.63	-566.1	-565.6	↓81
26.04.2010 15:12	-5.16 °N -23.11 °E	517.8	149.7	584.5	9.2	0.32	0.83	0.51	-654.0	-653.6	↓56
28.04.2010 13:54	1.78 °N -23.00 °E	540.9	144.4	619.8	-33.1	0.34	1.27	0.93	-682.1	-681.8	↓76
29.04.2010 14:21	4.99 °N -23.00 °E	562.8	114.2	615.9	-11.7	0.35	1.25	0.89	-575.4	-574.9	↓53
30.04.2010 14:15	8.07 °N -23.00 °E	550.6	118.6	591.1	-0.6	0.35	0.94	0.60	-680.8	-680.5	↓71
02.05.2010 14:39	14.55 °N -23.68 °E	541.3	110.5	603.3	-15.0	0.35	1.13	0.78	-680.7	-680.4	↓24
04.05.2010 13:39	17.61 °N -24.75 °E	523.2	121.5	686.5	-83.6	0.34	2.27	1.93	-630.8	-630.3	↓74
05.05.2010 13:21	20.26 °N -22.86 °E	559.0	125.7	667.9	-55.3	0.36	2.05	1.69	-572.6	-572.2	↓66
06.05.2010 12:30	23.12 °N -20.66 °E	550.7	104.3	586.6	-1.1	0.36	0.93	0.57	-719.3	-719.0	↓58
07.05.2010 12:18	26.07 °N -17.50 °E	539.8	108.9	575.3	20.3	0.35	0.79	0.43	-645.2	-644.8	↓21
09.05.2010 12:51	33.60 °N -13.86 °E	546.8	104.6	624.2	21.0	0.37	1.51	1.14	-327.2	-326.4	↓10
10.05.2010 12:55	36.53 °N -13.01 °E	531.8	107.8	571.6	62.0	0.36	0.77	0.41	-230.2	-229.3	↓13
09.02.2008 16:05	16.91 °N -16.82 °E	527.2	118.4	141.7	-224.09	0.35	1.57	1.22	-221.8	-221.0	↓46
11.02.2008 17:58	18.77 °N -16.81 °E	538.5	115.3	550.4	-383.39	0.36	5.91	5.54	-381.6	-380.9	↓628
15.02.2008 10:27	17.93 °N -16.38 °E	536.8	112.2	138.8	-114.85	0.36	1.79	1.42	-112.2	-111.3	↓92
16.02.2008 6:05	17.72 °N -16.69 °E	548.4	120.0	20.3	-180.51	0.37	0.50	0.13	-179.0	-178.2	↓35
16.02.2008 17:41	18.01 °N -17.01 °E	548.4	120.0	31.0	-218.73	0.37	0.72	0.35	-217.3	-216.5	↓94
18.02.2008 18:22	18.00 °N -23.00 °E	541.8	126.5	48.9	-321.61	0.36	1.16	0.80	-320.4	-319.7	↓22

- Sylvia Walter 20.12.2015 21:33
Deleted: supersaturation... aturation (1)
- Sylvia Walter 20.12.2015 21:33
Deleted: m
- Sylvia Walter 20.12.2015 21:33
Deleted: D_m
- Sylvia Walter 20.12.2015 21:33
Deleted: 3.75
- Sylvia Walter 20.12.2015 21:33
Deleted: 7.80
- Sylvia Walter 20.12.2015 21:33
Deleted: 7.41
- Sylvia Walter 20.12.2015 21:33
Deleted: 9.74
- Sylvia Walter 20.12.2015 21:33
Deleted: 4.81
- Sylvia Walter 20.12.2015 21:33
Deleted: 1.56
- Sylvia Walter 20.12.2015 21:33
Deleted: 2.76
- Sylvia Walter 20.12.2015 21:33
Deleted: 2.53
- Sylvia Walter 20.12.2015 21:33
Deleted: 1.71
- Sylvia Walter 20.12.2015 21:33
Deleted: 2.24
- Sylvia Walter 20.12.2015 21:33
Deleted: 5.74
- Sylvia Walter 20.12.2015 21:33
Deleted: 4.66
- Sylvia Walter 20.12.2015 21:33
Deleted: 1.58
- Sylvia Walter 20.12.2015 21:33
Deleted: 1.21
- Sylvia Walter 20.12.2015 21:33
Deleted: 3.10
- Sylvia Walter 20.12.2015 21:33
Deleted: 1.13
- Sylvia Walter 20.12.2015 21:33
Deleted: 3.46
- Sylvia Walter 20.12.2015 21:33
Deleted: 15.28
- Sylvia Walter 20.12.2015 21:33
Deleted: 3.92
- Sylvia Walter 20.12.2015 21:33
Deleted: 0.35
- Sylvia Walter 20.12.2015 21:33
Deleted: 0.94
- Sylvia Walter 20.12.2015 21:33
Deleted: 2.22

1 Figure captions

2 Figure 1: a) cruise tracks of the *RV Polarstern*, dots indicate positions of discrete atmospheric air sampling, b) positions of surface water
3 headspace sampling during ANT-XXVI/4 ($n = 16$, green dots) and the *RV L'Atalante* ATA-3 cruise ($n = 6$, black dots)

4 Figure 2: Experimental setup for headspace sampling, a) sampling of the surface water into the glass vessel, connected to the Niskin bottle
5 rosette, b) scheme of the experimental setup

6 Figure 3: Comparing the H_2 mole fractions [ppb] measured with the isotopic experimental setup (x-axis) and the Peak Performer 1 RGA (y-
7 axis) during ANT-XXVI/1 (red labeled) and ANT-XXV/5 (yellow labeled), $y = 0.979x + 3.96$, $R^2 = 0.81$, $n = 147$

8 Figure 4: $\delta D (H_2)$ [‰] (first column), H_2 mole fraction [ppb] (second column), and CO mole fraction [ppb] (third column), along the
9 meridional cruise tracks of *RV Polarstern*, the mole fraction and δD of H_2 are measured by IRMS, the CO mole fraction by RGA

10 Figure 5: Comparison of measurement results of H_2 and CO mole fractions and δD with TM5 model results (given in red). Data are shown
11 against latitude. The blue markers show results of flask samples, the green markers represent the continuous in-situ measurements
12 (performed with the peak performer instrument on-board). CO has not been analysed in the flasks sampled during the last cruise. The model
13 data were interpolated at the place and time of sampling or measurements.

14 Figure 6: a) H_2 mole fraction [ppb] (black) and δD [‰] (red) along the ANT-XXV/5 high-resolution transect $24^\circ S - 15^\circ S$; b) Keeling plot of
15 the samples along the high-resolution transect north of $18^\circ S$. The three trend lines indicate the range of the Keeling plot analysis that was
16 applied to determine the source signature.

17 Figure 7:
18 a) H_2 saturation in the surface water (color coded) along the *RV Polarstern* cruise track of ANT-XXVI/4 and the *RV L'Atalante* cruise ATA-
19 3, with maxima around the Cape Verde islands and $10 - 15^\circ S$, Note: each sample is represented by a single dot.
20 b) Comparing the $\delta D (H_2)$ at different water temperatures, the respective H_2 saturation are color coded, sample dots marked with a diamond
21 belong to the *RV L'Atalante* cruise, sample dots without to the ANT-XXVI/4 cruise; $y = -35.2x + 360.9$, $R^2 = 0.66$, $n = 22$
22 c) Distribution of $\delta D (H_2)$ (color coded) in correlation between water temperature and salinity
23 d) Correlation between water temperature and H_2 saturation, the $\delta D (H_2)$ is color-coded, the exceptional high saturation has been excluded
24 from the correlation calculation, $y = 0.26x - 2.79$, $R^2 = 0.22$, $n = 21$
25

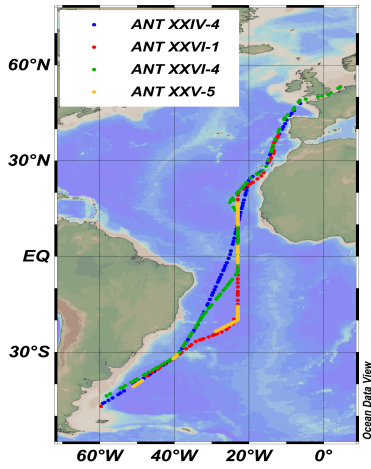
26 Figure 8: Oceanic H_2 emissions used in the TM5 model simulations ($mmol m^{-2} a^{-1}$, based on the distribution provided by the project GEMS
27 (Global and regional Earth-system (Atmosphere) Monitoring using Satellite and in-situ data) and scaled to a total oceanic source of $5 Tg a^{-1}$
28 (Pieterse et al. (2013))

29
30

- Sylvia Walter 20.12.2015 21:33
Deleted: supersaturation factor
- Sylvia Walter 20.12.2015 21:33
Deleted: note
- Sylvia Walter 20.12.2015 21:33
Deleted: factors
- Sylvia Walter 20.12.2015 21:33
Deleted: factor
- Sylvia Walter 20.12.2015 21:33
Formatted: Font:Times New Roman
- Sylvia Walter 20.12.2015 21:33
Formatted: Font:Times New Roman
- Sylvia Walter 20.12.2015 21:33
Formatted: Font:Times New Roman
- Sylvia Walter 20.12.2015 21:33
Formatted: Text, Justified, Line spacing: 1.5 lines
- Sylvia Walter 20.12.2015 21:33
Deleted: above 15
- Sylvia Walter 20.12.2015 21:33
Formatted: Font:Times New Roman
- Sylvia Walter 20.12.2015 21:33
Formatted: Font:Times New Roman
- Sylvia Walter 20.12.2015 21:33
Formatted: Font:Times New Roman
- Sylvia Walter 20.12.2015 21:33
Formatted: Font:Times New Roman

1

a)



b)

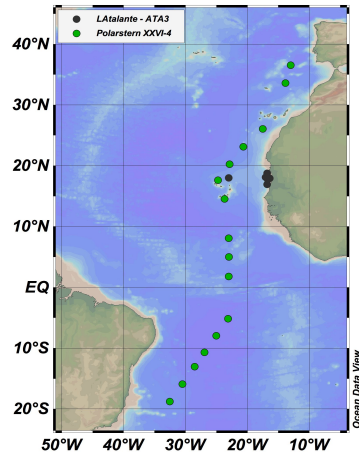


Figure 1: a) cruise tracks of the *RV Polarstern*, dots indicate positions of discrete atmospheric air sampling, b) positions of surface water headspace sampling during ANT-XXVI/4 ($n = 16$, green dots) and the *RV L'Atalante* ATA-3 cruise ($n = 6$, black dots)

2

3

4

Sylvia Walter 20.12.2015 21:33
Formatted: Line spacing: multiple 1.15 li

1

a)



b)

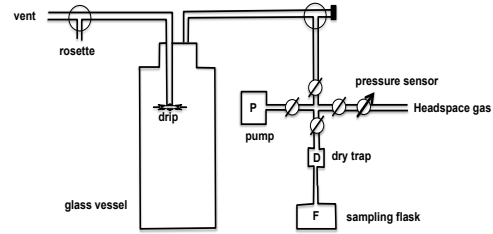


Figure 2: Experimental setup for headspace sampling, a) sampling of the surface water into the glass vessel, connected to the Niskin bottle rosette, b) scheme of the experimental setup

2

3

Sylvia Walter 20.12.2015 21:33
Formatted: Line spacing: multiple 1.15 li

1

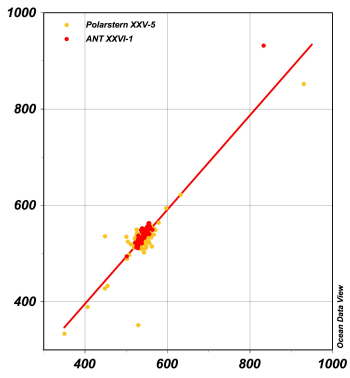


Figure 3: Comparing the H₂ mole fractions [ppb] measured with the isotopic experimental setup (x-axis) and the Peak Performer 1 RGA (y-axis) during ANT-XXVI/1 (red labeled) and ANT-XXV/5 (yellow labeled), $y = 0.979x + 3.96$, $R^2 = 0.81$, $n = 147$

2

3

Sylvia Walter 20.12.2015 21:33

Formatted: Normal, Left, Line spacing:
multiple 1.15 li

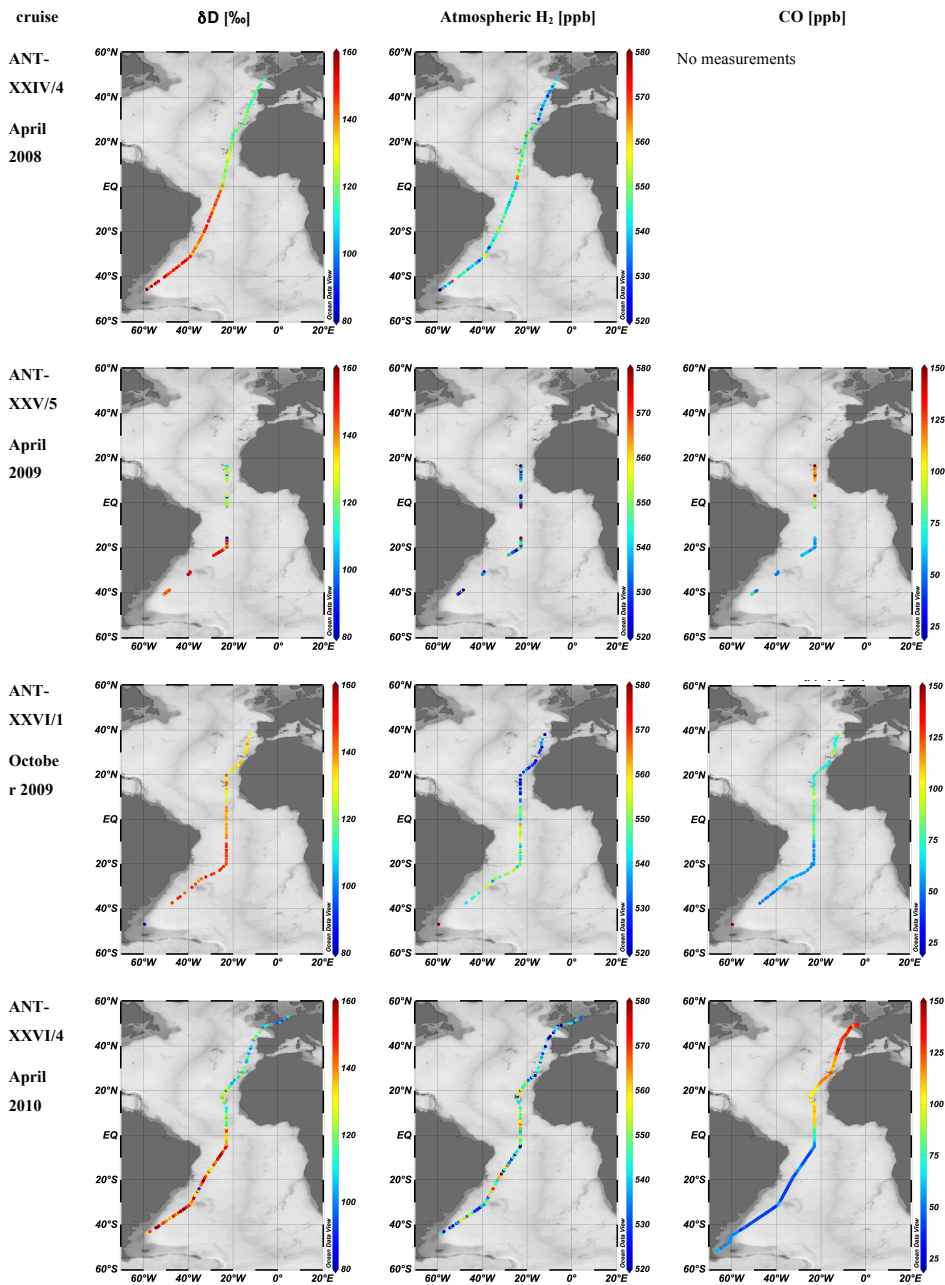


Figure 4: δD (H_2) [‰] (first column), H_2 mole fraction [ppb] (second column), and CO mole fraction [ppb] (third column), along the meridional cruise tracks of *RV Polarstern*, the mole fraction and δD of H_2 are measured by IRMS, the CO mole fraction by RGA

Sylvia Walter 20.12.2015 21:33
Formatted: Line spacing: multiple 1.15 li

1

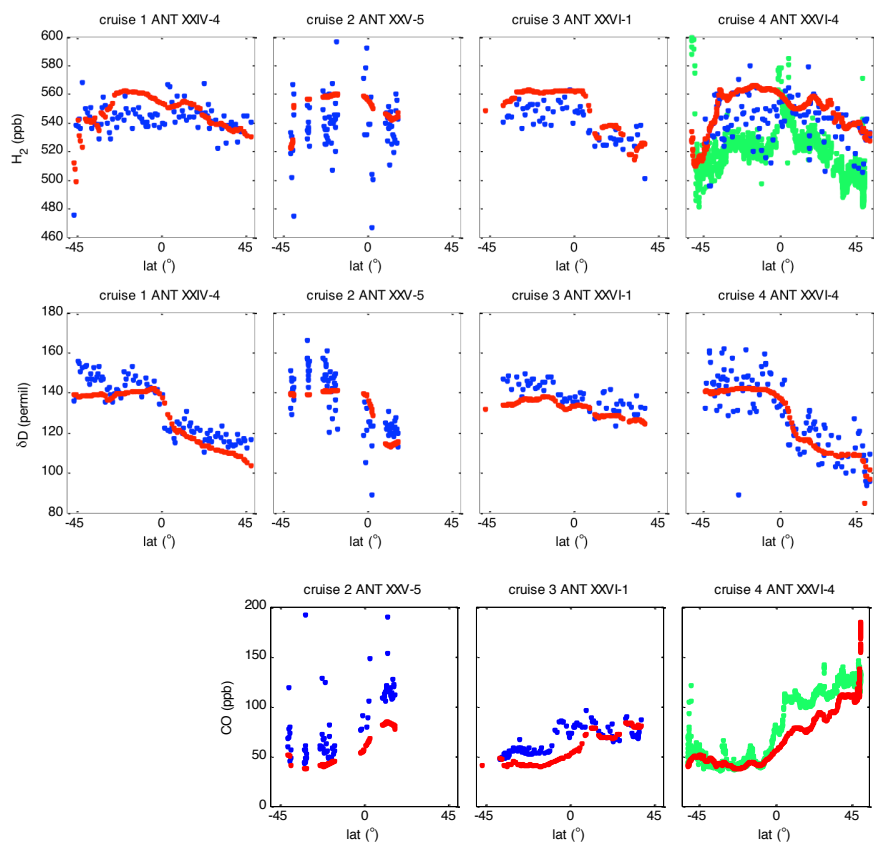


Figure 5: Comparison of measurement results of H_2 and CO mole fractions and δD with TM5 model results (given in red). Data are shown against latitude. The blue markers show results of flask samples, the green markers represent the continuous in-situ measurements (performed with the peak performer instrument on-board). CO has not been analysed in the flasks sampled during the last cruise. The model data were interpolated at the place and time of sampling or measurements.

2

3

Sylvia Walter 20.12.2015 21:33
Formatted: Line spacing: multiple 1.15 li

1

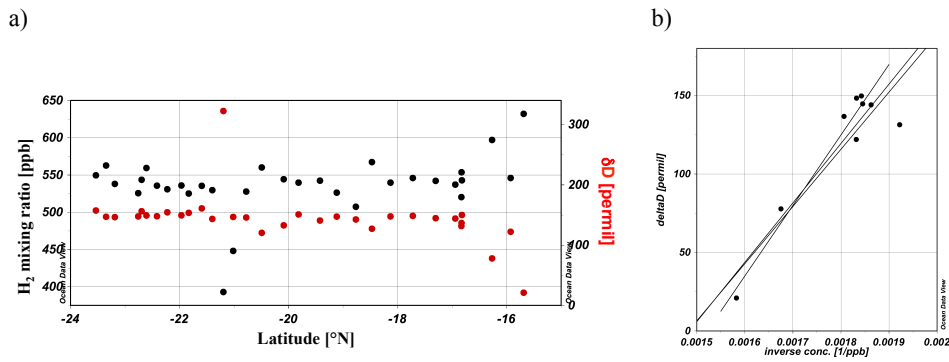


Figure 6: a) H₂ mole fraction [ppb] (black) and δD [‰] (red) along the ANT-XXV/5 high-resolution transect 24° S–15° S; b) Keeling plot of the samples along the high-resolution transect north of 18° S. The three trend lines indicate the range of the Keeling plot analysis that was applied to determine the source signature.

2

3

4

5

6

7

8

9

Sylvia Walter 20.12.2015 21:33
Formatted: Line spacing: multiple 1.15 li

1

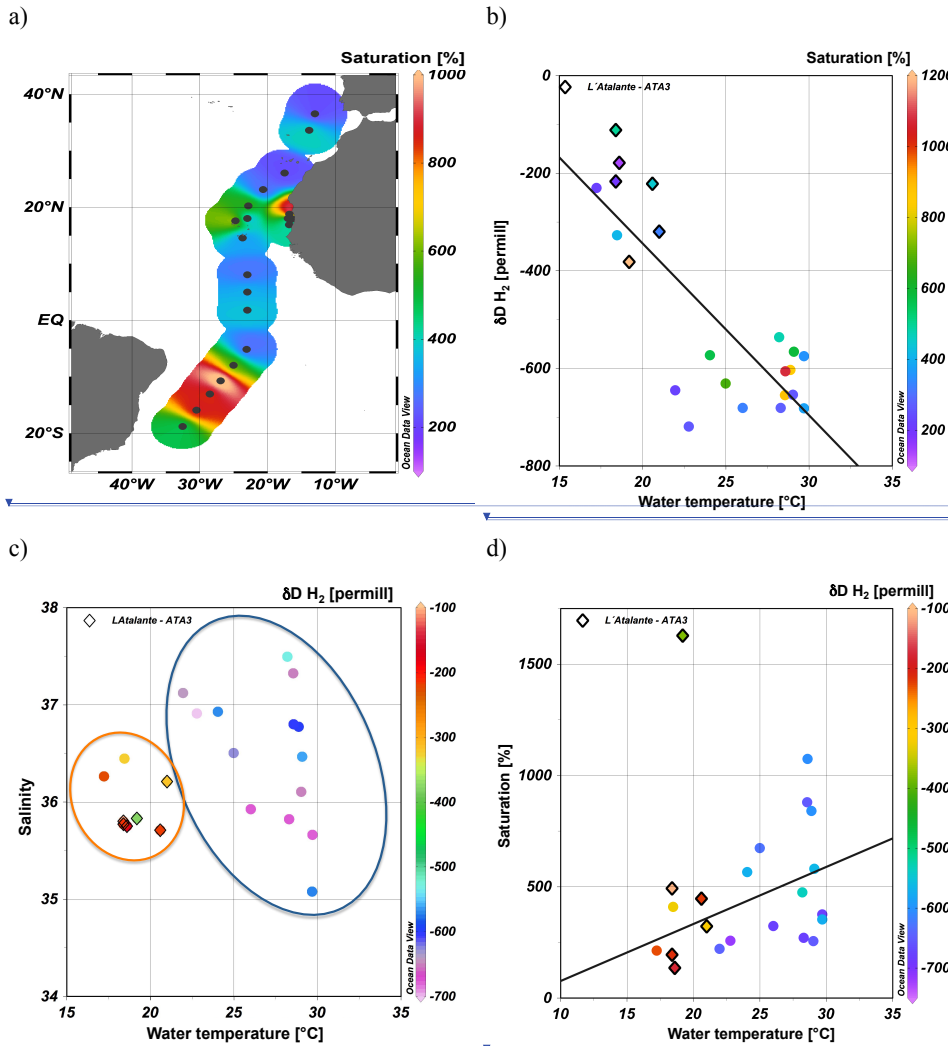
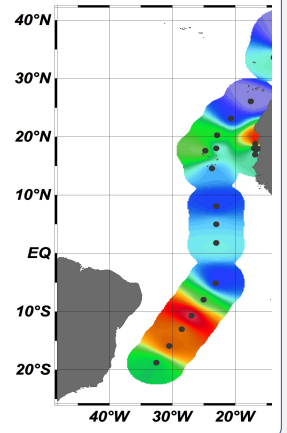


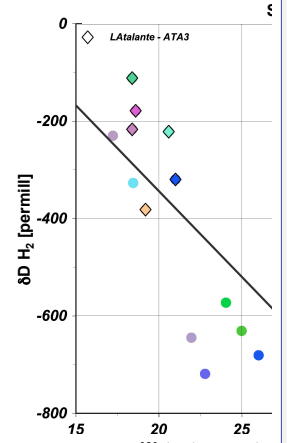
Figure 7:
 a) H_2 saturation in the surface water (color coded) along the RV *Polarstern* cruise track of ANT-XXVI/4 and the RV *L'Atalante* cruise ATA-3, with maxima around the Cape Verde islands and 10–15° S, **Note:** each sample is represented by a single dot.
 b) Comparing the $\delta D (H_2)$ at different water temperatures, the respective H_2 saturations are color coded, sample dots marked with a diamond belong to the RV *L'Atalante* cruise, sample dots without to the ANT-XXVI/4 cruise; $y = -35.2x + 360.9$, $R^2 = 0.66$, $n = 22$
 c) Distribution of $\delta D (H_2)$ (color coded) in correlation between water temperature and salinity
 d) Correlation between water temperature and H_2 saturation, the $\delta D (H_2)$ is color-coded, the exceptional high saturation has been excluded from the correlation calculation, $y = 0.26x - 2.79$, $R^2 = 0.22$, $n = 21$

2

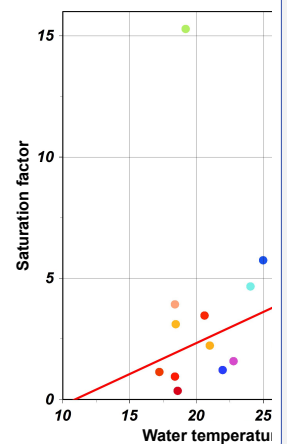
3



Deleted:
 Sylvia Walter 20.12.2015 21:33



Deleted:
 Sylvia Walter 20.12.2015 21:33



Deleted:
 Sylvia Walter 20.12.2015 21:33

Formatted: Line spacing: multiple 1.15 li

Sylvia Walter 20.12.2015 21:33

Deleted: supersaturation factor...atur ... [2]

Sylvia Walter 20.12.2015 21:33

Deleted: saturation factors

Sylvia Walter 20.12.2015 21:33

Deleted: factor... the $\delta D (H_2)$ is colc ... [3]

41

1

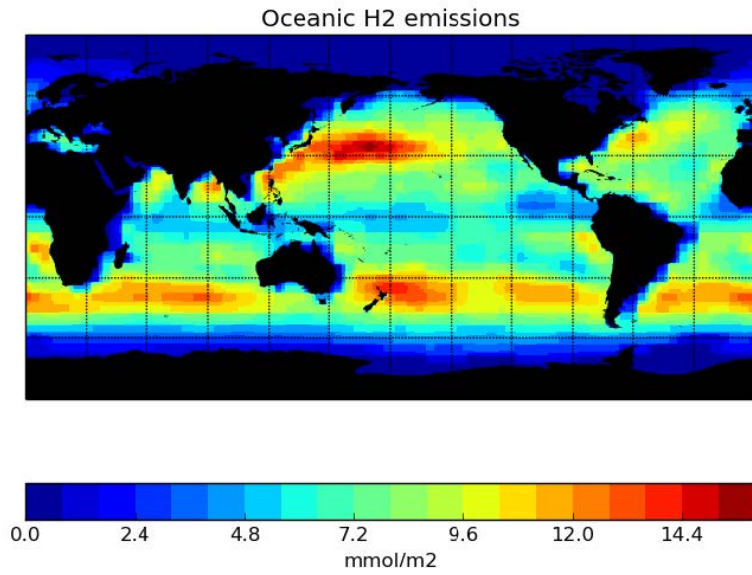


Figure 8: Oceanic H₂ emissions used in the TM5 model simulations ($\text{mmol m}^{-2} \text{a}^{-1}$, based on the distribution provided by the project GEMS (Global and regional Earth-system (Atmosphere) Monitoring using Satellite and in-situ data) and scaled to a total oceanic source of 5 Tg a^{-1} (Pieterse et al. (2013))

2

Sylvia Walter 20.12.2015 21:33
Formatted: Line spacing: multiple 1.15 li

Interactive comment on “Isotopic evidence for biogenic molecular hydrogen production in the Atlantic Ocean” by S. Walter et al.

S. Walter et al.

s.walter@uu.nl

Received and published: 20 November 2015

Dear referee, thanks for your comments. Please find our reply in-line. Kind regards, S. Walter

Major Comments: Page 16440-42, Section 2.4.3, diss. H₂ measurements: Since the extraction method is new and presented for the first time, I would like to see a discussion about the overall measurement errors of both the diss H₂ conc. and its isotope signature in seawater. Reply: The following discussion has been included in the manuscript: A new method has been presented to extract H₂ from surface waters for isotopic determination. Before discussing the measurement results, we will give an overview of the possible main errors and their effects. To show the effect of the errors

Full Screen / Esc

Printer-friendly Version

Interactive Discussion

Discussion Paper

on the measurements, we will present error factors, thus how much the final data differ by shifting the respective parameter by 1 % and also the absolute assumed error. For the extraction method several error sources could be identified: the determination of pressure, especially in the sampling vessel before adding the make-up gas and during extraction, the temperature of air and water, respectively the difference between them when the sample is extracted from the headspace, and the volume of the set-up and the sample. The determination of pressure in the sampling vessel would be one issue of further improvement, because the error caused by pressure deviations for the total pressure after adding the make-up gas is about a factor of 0.7 for concentrations and 0.2 for the isotopic values. The error based on temperature of air, water and sample is negligible due to high-precision measurements and the short handling time between water sampling and headspace extraction. The error for the volume parameter for the set-up is negligible due to the high volume, the precise determination of the glass vessel volume by weighing, and the calculation of the tubing volume. The main error source is the water volume of the sample, which counts by a factor of 5.9 for the concentration, but with negligible effect on the isotopic values. Although the relative error factor is quite high the absolute value is assumed to be around 0.5% due to the sample size, which has also been weighed at the home lab. The H₂ measurement procedure is the same as for atmospheric samples and possible errors are described in the respective sessions or related literature. However, the error caused by the determination of the dry mole fraction itself seems to have the main input by a factor of 5.3 for concentration and 4.6 for the isotopic values of dissolved H₂. Errors of the determination of the isotopic value are much less significant and count by a factor of 0.2. Taking measurement and handling errors during the extraction as well as errors in the determination of the dry mole fraction into account, we assume a robust standard deviation of $\pm 6.9\%$ for the dissolved H₂ mole fractions and $\pm 4.7\%$ for the isotopic values by calculating the root of the sum of the squared uncertainties. As shown in Table 4 we also tested the effect of equilibrium isotopic fractionation and kinetic isotopic fractionation. The effect is less than 0.2%. Therefore, recommendations for the extraction

[Full Screen / Esc](#)[Printer-friendly Version](#)[Interactive Discussion](#)[Discussion Paper](#)

method are to additionally measure parameters such as the initial pressure in the glass vessel and to ensure a precise determination of the sample volume. Besides this we recommend high-precision IRMS measurements and to consider multiple sampling for better statistics on the data. Absolute error assumptions: ΔT air-sea: 0.3% Pressure sensor: 0.5% Temperature air: 0.01°C Temperature water: 0.01°C V vessel: 0.5% V tubing: 10% IRMS measurements: 1%

p.16441, Eq.(6): H₂ solubility in seawater is also depending on the salinity, thus, I am wondering why the 'salt effect' is not considered in Eq.6. Reply: The actual salinity has been taken into account in the concentration calculations.

p.16441, l. 16; Eq.(7); p.16449, l.6: The extraction efficiency is given as 92%. Is this a mean value? The extraction efficiency according to Eq.(7) is depending on the Ostwald solubility coefficient which, in turn, depends on the temperature. Was the temperature always the same? Please give details. Reply: the mean value is 92.12 (± 0.013)%. Due to the very low variation we mentioned just one value without decimal places. We included this to the manuscript for completeness.

p.16441, l.16: Please cite a reference for the Ostwald coefficient. Reply: we included a reference for the Ostwald coefficient.

p.16448, l.13-15: '. . . possibilities for improvements ...' are mentioned. However, what does that mean for the analytical error of the presented data? Or in other words are they just by chance in agreement with the literature data? Reply: The possible improvements include a better monitoring of additional data such as temperature and pressure in the vessel itself, this was not possible yet. As already mentioned in chapter 2.3, the temperature dependence of the H₂ solubility is quite low with less than 0.3% per K, and also the used pressure sensors (Omega, PAAR21R) work within a low error range of 0.5% or even below. In combination with the high extraction efficiency and the standardized sampling procedure over the two cruises, we are convinced that the presented data sets are comparable and not just by chance in agreement with the

[Full Screen / Esc](#)[Printer-friendly Version](#)[Interactive Discussion](#)[Discussion Paper](#)

literature data. Please see the discussion about possible error sources above.

Table 4: I was surprised to see a positive (i.e. excess) H₂ concentration differences resulting in undersaturations of 0.35 and 0.94. That does not seem to be logical at all: How can a concentration excess of H₂ result in a H₂ undersaturation? Please explain.

Reply: We gave the supersaturation factor, but changed this to saturation in % as also suggested by referee #2 to avoid misunderstandings.

Discussion of oceanic sources of H₂ (see Section 3.3.1; Table4; Figure7): It is obvious that the majority of H₂ data pool associated with the low temperatures has been measured in the coastal upwelling system off Mauritania. Upwelled waters off Mauritania, however, are originating from water depths down to 150-200m (i.e. upper oxygen minimum zone, OMZ). Thus, it is not that surprising to see a different H₂ signature because in OMZ waters there might different sources/sinks at work: E.g., the interplay between H₂ production (i.e. by N₂ fixation at depth) and associated H₂ oxidizing bacteria (which live at oxic/anoxic interfaces in particles and sediments). Reply: We showed in Walter et al. 2012, that bacteria and algae species with quite different H₂ pathways (*C. saccharolyticus*, *A. brasiliensis*, *E. coli*, *C. acetobutylicum* and *C. reinhardtii*) produce H₂ with similar, highly depleted isotopic signatures of around -700 ‰. The tested species included a N₂-fixer as well as fermentative bacteria and also a limnic green alga. As mentioned (Chen et al. 2015) an isotopic enrichment causing a shift of almost 400‰ just by removal of H₂ is unlikely due to unrealistic large fractions needed to be removed. Although OMZ waters and borders are known as microbial very active areas and we therefor cannot exclude such high turn-over rates completely, we assume another source responsible for the differing isotopic signature. As suggested in Walter et al. 2013, photochemical degradation of VOCs could play a role. The up-welling areas are quite productive and could indirectly emit pre-cursors of H₂. Unfortunately, up to now there are no data available about the isotopic signature of photochemically produced H₂ in surface waters. The value given for atmospheric photochemically produced H₂ is around +100 to +200‰ and would fit to this hypothesis.

BGD

12, C7842–C7846, 2015

Interactive
Comment

Full Screen / Esc

Printer-friendly Version

Interactive Discussion

Discussion Paper

C7845



Moreover, I am not really convinced by the argument against a H₂ sink (see p.16451, lines 1-5) since the observed undersaturations point towards a net H₂ sink (sink > source) they can, therefore, not result from a single source (see p.16451, l.17-20).
Reply: We changed from reporting the supersaturation factor to the saturation to avoid misunderstandings.

Technical Comments: Mauretania should read Mauritania, please check spelling throughout the manuscript. Reply: spelling has been checked and corrected

Table 4: X_h and D_a are mentioned in the table caption, but do not appear in the header of the table: I guess that X_m and D_m should read X_h and D_a (or the other way round).
Reply: this has been corrected

p.16439/40; Figures 4 and 5: Please remove the CO data when they are not essential for the discussion of the H₂ data
Reply: The CO data are indeed not essential for this publication, but CO data are used to model H₂ emissions caused by N₂ fixation. We therefore prefer to keep them in as general information, although we do not discuss them in detail.

Suppl. Material: There are citations in the text of the Supplement, but there is no list of references. Please add list with full references. Reply: we added the reference list.

Interactive comment on Biogeosciences Discuss., 12, 16431, 2015.

[Full Screen / Esc](#)[Printer-friendly Version](#)[Interactive Discussion](#)[Discussion Paper](#)

Interactive comment on “Isotopic evidence for biogenic molecular hydrogen production in the Atlantic Ocean” by S. Walter et al.

S. Walter et al.

s.walter@uu.nl

Received and published: 20 November 2015

Dear referee, thanks for your comments. Please find our reply in-line. Kind regards, S. Walter

p. 16441 l. 16-17: How exactly was the value of 92 % for the extraction efficiency determined? Is this a mean for all samples? What was the variability for the whole dataset? Reply: the mean value is 92.12 (± 0.013)%. Due to the very low variation we mentioned just one value without decimal places. We included this to the manuscript for completeness.

p. 16448 l. 13-15: Please detail planned/recommended improvements and expected impact on measurements. Reply: The possible improvements include a better monitor-

Full Screen / Esc

Printer-friendly Version

Interactive Discussion

Discussion Paper



ing of additional data such as temperature and pressure in the vessel itself, this was not possible yet. As already mentioned in chapter 2.3, the temperature dependence of the H₂ solubility is quite low with less than 0.3% per K, and also the used pressure sensors (Omega, PAAR21R) work within a low error range of 0.5% or even below. In combination with the high extraction efficiency and the standardized sampling procedure over the two cruises, we are convinced that the presented data sets are reasonable. A more detailed discussion about uncertainties and their effect on the results has been added to the manuscript (see also reply to referee #1).

p. 16452 l. 21: Ist he global nitrogen fixation rate of 175 TgN a⁻¹ a result from the GEMS database? Reply: This was a typo, it should have been the value given by Großkopf et al. (2012). The value has been corrected.

Table 2: Why were samples excluded? Were there any issues with the sample handling or contamination? Reply: 5 samples out of almost 200 were excluded as outliers (>2 σ), however, we do have no explanation for the deviation. There was no indication for sampling or measurement errors.

Technical comments Consider reporting saturations in % instead of saturation factors/supersaturation throughout the manuscript to facilitate comparison with other publications. Reply: we changed the supersaturation factor to saturation.

Table 4: Caption differs from table headings for xh/xm, Da/dDa and Dh/dDm Reply: This has been corrected.

Supplement p. 2: Format citation for Green Carritt, 1967, add full reference to supplement. Reply: the full reference has been added and formatted

Supplement p. 4: Add full reference for Knox et al., 1992. Reply: the full reference has been added

Interactive comment on Biogeosciences Discuss., 12, 16431, 2015.